The Thesis Committee for Lindsey A. Sydow
Certifies that this is the approved version of the following thesis:

Cinder Pool's Sulfur Chemistry: Implications for the Origin of Life in Hydrothermal Environments

APPROVED BY
SUPERVISING COMMITTEE:

Supervisor:

Philip C. Bennett

M. Bayani Cardenas

Daniel O. Breecker

Cinder Pool's Sulfur Chemistry: Implications for the Origin of Life in Hydrothermal Environments

by

Lindsey A. Sydow B.S.

Thesis

Presented to the Faculty of the Graduate School of

The University of Texas at Austin

in Partial Fulfillment

of the Requirements

for the Degree of

Master of Science in Geological Sciences

The University of Texas at Austin

August 2013

Dedication

I dedicate my thesis to all of my loved ones who helped me reach this point of its momentous publication.

Acknowledgements

I would like to thank first and foremost the Jackson School for funding my education. Special thanks go to Kirk Nordstrom, Blaine McCleskey, Jim Ball, Kate Campbell, and Randall Chiu of the USGS for their incredible help at Yellowstone and subsequent collaboration, as well as Greg Druschel and Angel Garcia of the University of Vermont and Will Wolfe. Also a huge thank you to Chris Oswalt for constructing Figure 4, and for so many other things that can't be quantified. Finally, thanks to Phil and the rest of the Bennett Lab for their invaluable assistance and encouragement over the last 3 years.

Abstract

Cinder Pool's Sulfur Chemistry: Implications for the Origin of Life in Hydrothermal Environments

Lindsey A. Sydow, M.S. Geo. Sci.

The University of Texas at Austin, 2013

Supervisor: Philip C. Bennett

One chemoautotrophic origin of life theory posits the abiotic formation of alkyl thiols as an initial step to forming biomolecules and eventually a simple chemoautotrophic cell. The premise of this theory is that a recurring reaction on the charged surfaces of pyrite served as a primordial metabolism analogous to the reductive acetyl-CoA pathway (Wächtershäuser 1988) that was later enveloped by a primitive cellular membrane. Alkyl thiols have not previously been identified in terrestrial hot springs as unequivocally abiogenic, but they have been produced in the laboratory under hydrothermal conditions in the presence of a catalyst.

I analyzed the dissolved gas content of several hot springs and conducted sterile laboratory experiments in order to evaluate the abiogenic formation of methanethiol (CH_3SH), the simplest of the alkyl thiols. Specifically of interest was Cinder Pool, an acid-sulfate-chloride hot spring in Yellowstone National Park. This spring is unusual in that it contains a subaqueous molten sulfur layer (~18 m depth) and thousands of iron-

sulfur-spherules floating on the surface, which are created by gas bubbling through the molten floor of the spring. This material could potentially serve as a reactive and catalytic surface for abiogenic CH_3SH formation in Cinder Pool.

Gas samples were collected from Cinder Pool and an adjacent hydrothermal feature in fall of 2011 using the bubble strip method. Two samples contained measurable quantities of CH_3SH and other organic sulfur gases, with concentrations of all gases generally higher at the bottom of the pool. Laboratory microcosm experiments were conducted to replicate these findings in a sterile environment. Analog Cinder Pool water was injected into serum bottles containing different iron-sulfur compounds, including cinders collected from the pool itself, as catalytic surfaces for the CH_3SH generating reaction. The bottles were then charged with hydrogen (H_2), carbon dioxide (CO_2), and carbon disulfide (CS_2) as reaction gases and incubated for a week at temperatures between 60 and 100^{o}C. Bottles used either powdered FeS, FeS_2 (pyrite) or cinder material as a catalytic surface, and all of these surfaces were capable of catalyzing CH_3SH formation. In bottles without imposed CS_2, however, cinder material was the only surface that produced any detectable CH_3SH.

While CH_3SH is central to the autotroph-first theory and has been synthesized in the laboratory (e.g. Heinen and Lauwers 1996), it has not previously been observed to form abiotically in natural systems. I have identified CH_3SH in a natural hydrothermal feature where it is unlikely to have formed secondary to microbial activity, and I have duplicated these field findings in sterile laboratory experiments using the cinders as a reactive surface for formation.

Table of Contents

List of Tables

List of Figures

Chapter 1: Introduction

1.1 The Origin of life

The question of how the first life may have developed on Earth and what form it took has been perplexing humankind for its entire existence. Scientifically based theories, however, have largely arisen in the last century and can generally be divided into two categories: autotroph-first and heterotroph-first. Heterotroph first models are based on the idea that building blocks of life such as amino acids formed abiotically in a "primordial soup," while autotroph-first models suggest that a primitive autotrophic metabolism is a necessary precursor to life (Konhauser 2007). Proponents of both models, however, generally agree that life emerged in the Archean eon between 4.0 and 3.8 Ga.

The first experiments testing a mechanism for abiotic production of organic material came from Miller and Urey in the early 1950s. These experiments sought to demonstrate the previously hypothesized abiotic formation of a primordial soup in the presence of a highly reducing atmosphere (Oparin and Morgulis 1938; Urey 1952). Amino acids were generated from an electrically stimulated reaction between inorganic compounds expected in an acidic Hadean ocean and a simulated atmosphere of CH_4, NH_3, H_2O, and H_2 (Miller 1953; Miller and Urey 1959). The organic molecules generated would become both the building blocks of a simple cell, and food for the first heterotrophic organism.

Heterotrophs might be considered simpler life forms than autotrophs in that they merely have to absorb and break down organic molecules for energy rather than creating them, and therefore hold some appeal conceptually as the first organism. However, there are some important considerations about a heterotroph-first scenario. First, it necessitates the presence of a highly reducing atmosphere that may not have existed. Although the oxygen-free Archean atmosphere has been a generally accepted idea since the 1950s, the actual chemistry of the atmosphere at that time has been fiercely debated (Dimroth and Kimberley 1976; Law and Phillips 2006). Furthermore, in the event that a reducing atmosphere allowed for the formation of amino acids, the amount generated would have to be substantial in a vast ocean where there are few mechanisms near the surface to concentrate these compounds.

The idea of an autotrophic origin of life has received increasing attention since the 1977 discovery of thriving hydrothermal vent communities on the Galapagos Rift with chemoautotrophic microorganisms at the base of the food web. The "Iron-Sulfur World" hypothesis proposed a mechanism for the first metabolism to evolve from autocatalytic reactions on the positively charged surfaces of pyrite in these hydrothermal environments (Wächtershäuser 1990a; Wächtershäuser 1988a; Wächtershäuser 1988b). The pyrite (FeS_2) would serve as a catalytic surface to concentrate reactants, making their widespread abundance unnecessary, and the required reduced gases would be supplied by the vents and subsequent reactions with the surroundings. Because the release of available energy is necessary for subsequent cell functions, this model argues that a

"surface metabolism" logically precedes the existence of the cellular membrane and genetic machinery (Wächtershäuser 1990a; Wächtershäuser 1988b).

The surface metabolism would have begun with energy derived from precipitation of FeS_2 through the exergonic reaction of FeS and H_2S gas (both ubiquitous in hydrothermal environments) in aqueous solution. FeS_2 precipitation occurs via the oxidation of FeS (Drobner et al. 1990) in reaction (1):

$$FeS + H_2S(aq) \rightarrow FeS_2 + 2H_2 \qquad \Delta G^{0'} = -39.4 \text{ kJ/mol at } 100^oC \qquad (1)$$

The energy produced by this reaction provides reducing power for other reactions on the pyrite surface (Huber and Wächtershäuser 1997).

The hypothesized surface metabolism should ideally resemble a metabolism observed in extant life forms if it served as a precursor to the first life. One possibility is a primitive version of the reductive acetyl-CoA pathway leading to the reductive citric acid cycle (Huber and Wächtershäuser 1997; Wächtershäuser 1990b), observed today only in certain obligate anaerobes. Some anaerobic microorganisms that use the reductive acetyl-CoA pathway have isotope fractionation patterns indicating that they may have been the first autotrophs of extant species (Ragsdale 1991).

The reductive acetyl-CoA pathway depends on catalysis by acetyl-CoA synthase (which contains a Ni-Fe-S reaction center) to join carbon monoxide (CO) and coenzyme A (a thiol) into acetyl-CoA, a thioester which then enters the citric acid cycle:

$$HS\text{-}CoA + CH_3 + CO \xrightarrow[\text{acetyl-CoA synthase}]{} \text{acetyl-CoA} + H \qquad (2)$$

A primitive version of this pathway, substituting simple bimodal Ni-Fe-S clusters for acetyl-CoA synthase and methanethiol (CH_3SH) for the more complex coenzyme A, was

tested in laboratory experiments and produced thioacetic acid (CH_3COSH) via reaction (3) (Wächtershäuser 2007).

$$CH_3SH + CO \xrightarrow{\text{bimodal Ni-Fe-S}} CH_3COSH \quad (3)$$

This thioacid could then enter the reverse citric acid cycle to synthesize pyruvate, serving the purpose of the thioester acetyl-CoA in extant metabolisms (Cody 2000; Wächtershäuser 2007; Wächtershäuser 1990b).

There is potential for this process to occur in hydrothermal settings, as CO gas and transition metal sulfides like those substituted for acetyl-CoA synthase in the above experiment are common in hydrothermal environments. However, the abiotic synthesis of alkyl thiols such as CH_3SH is less certain. Because CH_3SH would have performed such a critical function in the proposed surface metabolism, its prebiotic and spontaneous formation is necessary for the advent of a surface metabolism.

1.2 Sterile Synthesis of Methanethiol

Methanethiol (CH_3SH) is a reduced organic sulfur compound and is the simplest of the thiols, all of which contain a carbon-bonded sulfhydryl group (SH). Previous research has attempted to determine if CH_3SH can form in the conditions common to hydrothermal environments. In sterile laboratory experiments, two scenarios for CH_3SH generation were tested at various temperatures in anaerobic conditions (Heinen and Lauwers 1996). In one system (an H_2S generating system) FeS, HCl, and CO_2 were incubated together and in the other FeS, H_2S, and CO_2 were incubated together. Thiols were generated in both scenarios in accordance with reaction series (4-6), with the

dominant product being CH_3SH at 75°C (Heinen and Lauwers 1996). The system with imposed H_2S began with reaction (5).

$$4FeS + 8HCl \rightarrow 4FeCl_2 + 4H_2S \quad (4)$$

$$3FeS + 3H_2S \rightarrow 3FeS_2 + 3H_2 \quad (5)$$

$$CO_2 + H_2S + 3H_2 \rightarrow CH_3SH + 2H_2O \quad (6)$$

In this case, the hydrogen is supplied by the formation of pyrite (Reaction 1), and serves as the reductant in thiol synthesis. If there is not enough hydrogen present in the system, CO_2 cannot be reduced for thiol generation. In an aqueous environment at 90°C with no H_2, CH_3SH concentration decreased over time, indicating its formation in natural hydrothermal systems may be hydrogen limited (Heinen and Lauwers 1996). Also observed in this experiment was dimethyl disulfide (DMDS, $(CH_3)_2S_2$), which is an oxidation product of CH_3SH, and carbon disulfide (CS_2). CS_2 is formed in this environment as an intermediate in reaction (6) that may persist depending on temperature and the ratio of FeS to H_2S. Reaction (6) can therefore be broken down into (6a) and (6b), with (6b) being the limiting step that requires catalysis for the formation of CH_3SH (Gutiérrez et al. 2011; Rushdi and Simoneit 2005).

$$CO_2 + 2H_2S \rightarrow CS_2 + 2H_2O \quad (6a)$$

$$CS_2 + 3H_2 \rightarrow CH_3SH + H_2S \quad (6b)$$

The H_2S produced in reaction (6b) could then react as in reaction (5) to produce more H_2, thus propagating the formation of more CS_2 and/or CH_3SH under the appropriate conditions. CS_2 has been observed in trace amounts in various hydro- and geothermal environments such as the Mount St. Helens ash plume and (tentatively) the headspace

above drill cores from the Escanaba Trough hydrothermal system (Rushdi and Simoneit 2005).

In addition to generation by the reduction of CO_2 as described in reaction (6), CH_3SH can also be formed through the reduction of CO (reaction 7), which requires less H_2 for the same amount of final product (Schulte and Rogers 2004).

$$CO + H_2S + 2H_2 \rightarrow CH_3SH + 2H_2O \quad (7)$$

While this reaction would theoretically yield higher thiol concentrations than reaction (6), the fugacity of CO is generally less than that of CO_2 in natural systems (Schulte and Rogers 2004), although they are frequently both observed in hydrothermal settings. However, CO may have played a more significant role in redox reactions during the Archean, as estimates of the atmospheric CO to CO_2 ratio are generally thought to be higher than they are today (Schulte and Rogers 2004).

Both CO and CO_2 dependent experiments yielded detectable CH_3SH, CS_2, and DMDS under simulated hydrothermal conditions (Heinen and Lauwers 1996; Schulte and Rogers 2004). With transition metal sulfides and CO (both of which are required compounds for the theorized surface metabolism) often found in these environments, the confirmation of abiotic CH_3SH generation under similar conditions greatly strengthens the idea that the first life would have been a hyperthermophilic chemoautotroph. However, these findings still require identifying abiogenic CH_3SH in a natural hydrothermal system.

1.3 METHANETHIOL IN THE ENVIRONMENT

CH_3SH appears as a common intermediate and byproduct of microbial metabolisms in ocean sediments and swamps or wetlands along with a related compound, dimethyl sulfide (DMS, H_3CSCH_3). Microbial oxidation of both CH_3SH and DMS influences sulfur flux in the atmosphere, as the oxidized byproducts are released as waste by the organisms (Lomans et al. 1997). CH_3SH specifically is the sole source of energy for certain methanogens that are also obligate methylotrophs that must oxidize compounds with a single carbon for energy (Konhauser 2007; Lomans et al. 1999). This metabolism has been referred to as a "throwback" to the earliest life on Earth (Huber and Wächtershäuser 1997).

Although observed in many biological systems, CH_3SH of unambiguously abiotic origin has not been identified in hydrothermal environments. However, the detection of CH_3SH and other thiols in sterile experiments designed to simulate hydrothermal environments suggests that they are likely present in these systems (Heinen and Lauwers 1996; Rushdi and Simoneit 2005; Schulte and Rogers 2004). Recently sampled vent waters from the Logatchev hydrothermal field (15^oN, 45^oW) revealed the presence of both methanethiol and propanethiol (Dias et al. 2010). While these gases could be abiotic in origin, the presence of diverse communities at this locale makes identifying them as such difficult. CH_3SH has also been identified in fluid inclusions from Archean aged quartz, which were analyzed by gas chromatography after crushing in a compartment connected to the chromatograph and direct flushing by a carrier gas into the detector

(Bray et al. 1991). These findings support the potential role CH_3SH may have played in the iron-sulfur world.

1.4 RESEARCH QUESTIONS

While successful abiogenic synthesis of CH_3SH in the laboratory under hydrothermal conditions answers the question of whether it *can* form abiotically in natural environments, it fails to answer the question, "*does* it?" And previously sampled hydrothermal systems host diverse microbial communities that make it difficult to answer this question with certainty. These sites are also typically located at the bottom of the ocean and thus are not easily accessible for this study. In an effort to identify abiogenic CH_3SH in a natural hydrothermal system, the following questions were addressed:

1) Is there a terrestrial hydrothermal site that contains the required reactants for abiotic CH_3SH formation, but where microbially mediated production is unlikely?
2) Can dissolved CH_3SH be detected in this environment?
3) Can abiotic synthesis of CH_3SH be replicated in the laboratory under sterile conditions by using only materials found in the identified hydrothermal site?

Chapter 2: Materials and Methods

2.1 Field Site Description

Cinder Pool is an acid-sulfate-chloride hydrothermal spring in the One Hundred Spring Plain of Norris Geyser Basin, Yellowstone National Park, Wyoming (44°43'57.16" N 110°42'35.21" W) (Figures 2 and 3). The name originates from the black sulfur spherules or "cinders" that float on the surface. The source of the cinders is a subaqueous layer of molten elemental sulfur at the bottom of the ~18 m deep pool. Gases bubble up through this layer and are encapsulated by the liquid sulfur material, which cools and solidifies as the bubble floats to the surface (Figure 4). Cinders are ~ 5 mm in diameter (Figure 5), and previous analysis has found that in addition to elemental sulfur (S^0) the cinders also contain iron dominantly in the form of pyrite, which gives the cinders their black color (Xu et al. 2000). Cinder Pool also has some of the most dynamic sulfur chemistry in the park, with concentrations of various constituents changing sometimes on an hourly basis. The pH generally fluctuates between 4 and 4.5, and the temperature is approximately 90^{o}C at the surface and 118^{o}C in the subaqueous sulfur at the bottom (Xu et al. 2000).

This environment, specifically the presence of potentially catalytic iron sulfide compounds in the molten sulfur material and the floating cinders, presents a unique opportunity to study a possible location for natural abiotic CH_3SH generation. The mild acidity of the pool as well as its high temperature and volcanic gas content fit the other additional criteria described by others (Heinen and Lauwers 1996; Wächtershäuser 1988b).

The only microorganism identified to date in Cinder Pool is *Aquificales Hydrogenobaculum* (Spear et al. 2005). This bacteria is a hydrogen and sulfur oxidizer, so it oxidizes reduced sulfur compounds and could potentially use CH_3SH as a substrate, but would not form it as a metabolic byproduct (Hügler et al. 2007; Reysenbach et al. 2009). It is also unlikely that this organism would be present at the bottom of the pool near the molten S^o. This limited biological community makes Cinder Pool a unique place to search for abiogenic CH_3SH outside of the lab.

2.2 FIELD SAMPLING

Dissolved gas samples to be analyzed using gas chromatography were taken from Cinder Pool and a number of other hydrothermal features in Norris Geyser Basin using the bubble strip method modified for use in hydrothermal settings (Mcinnes 2003). This technique uses a peristaltic pump to continuously flow water from the sample depth through an inverted 250 mL media bottle containing approximately 175 mL of solution and 75 mL of headspace for 30 minutes (Figure 6). During this time, the ~75 mL headspace in the bottle equilibrated with the gases originally dissolved in the water. Once equilibrated, the bottle was turned right side up and the bubble extracted with a gas-tight syringe. A small amount of this sample (0.5 mL) was injected directly into the gas chromatograph (GC) for preliminary on-site analysis, and then most of the sample was injected to a positive pressure into a dry, sterilized, and pre-evacuated 60 mL serum bottle for later analysis in the laboratory. These bottled samples were stored in the dark to minimize degradation caused by photo oxidation and were analyzed in the laboratory

approximately 10 days after their collection. Bubble stripped samples were collected from 1, 2, 3, 10, 17, and ~18 m deep within Cinder Pool.

During collection of the dissolved gas samples, collaborators from the USGS recorded unstable parameters and collected filtered water samples for chemical analysis of dissolved constituents in the laboratory. Samples for dissolved metal analysis were preserved using nitric acid, and the metal concentrations were determined using Inductively Coupled Plasma Mass Spectroscopy (ICP-MS). Dissolved anions were determined by High Performance Liquid Chromatography (HPLC). Values obtained from this analysis were later used to produce a synthetic Cinder Pool water for use in laboratory experiments.

Finally, cinders were collected for structural and elemental analysis in the laboratory as well as for use in experiments. Falcon tubes were used to skim floating cinders off the surface of the water near the edges of the pool. Some of the molten material from the bottom of the pool was also collected when the bubble strip's pump tubing sank below the water/sulfur interface while sampling at 18 m, inadvertently bringing up some of the molten material with the tube (Figure 7). To prevent oxidation of the iron in this material, it was stored in an anaerobic chamber with a constant 10% CO_2 and H_2 mix in N_2. Raw, unfiltered water was also taken from the pool for laboratory experiments.

2.3 Sulfur Gas Stability and Degradation Experiments

Sulfur gas stability experiments were conducted to gain preliminary insight into reactions between gases during sample storage as quality assurance for the field samples. Evacuated 60 mL serum bottles were filled to a positive pressure with a 1:1 dilution of 100 ppm sulfur gas standard (H_2S, COS, CH_3SH, and CH_3CH_2SH) with either nitrogen (N_2) , dry air, or air with 1 mL of synthetic Cinder Pool water to simulate the effects of moisture entering the syringe during bubble stripping. All bottles were then pressurized to ~0.7 atm above ambient with N_2 to ensure multiple samples could be pulled throughout the experiment. Degradation under each of these conditions was further explored by storing one bottle in the dark and one in direct sunlight during the daylight hours to examine photo oxidation effects. Complete darkness was accomplished by wrapping each of the dark bottles in foil and storing in a dark cabinet. Samples from each bottle were analyzed with the GC immediately on the day of bottling, after 24 hours, after 7 days, and after 18 days had elapsed.

2.4 Pool Microcosm Experiments

To recreate the reactions occurring in Cinder Pool, a series of experiments using 60 mL serum bottles as a microcosm for the pool were performed in the laboratory. Using dissolved constituent values obtained from Xu et al. (2000), a synthetic Cinder Pool water was prepared for use in experiments performed prior to obtaining these data directly from Cinder Pool during field sampling. After reagents were added to reach the appropriate ion concentrations, the liter of solution was titrated with 620 μL of 1 N HCl

to a pH of ~4. These experiments examined whether or not S^0 alone would allow for the abiotic formation of CH_3SH. They used bottles with ~4 g of S^0 in 30 mL of either synthetic Cinder Pool water or dilute HCl (also with a pH of approximately 4) and were given a headspace of 66% H_2 and 33% CO_2 at a total pressure of 2 atm. The bottles were incubated in an autoclave at 121°C for at least 12 hours overnight. These experiments were initially performed under semi-aerobic conditions, meaning the headspace imposed on the bottles contained no oxygen while the media contained dissolved oxygen, and were later repeated completely anaerobically.

To recreate the reaction mechanism using FeS proposed by Heinen and Lauwers (1996), 10 mL of synthetic Cinder Pool water or dilute HCl, 0.1-0.14 g of FeS, and a 1.4 atm headspace of 100% CO_2 were allowed to incubate overnight in the autoclave at 121°C. The purpose of omitting the H_2 in the headspace was to determine if enough could be produced via reaction (3) to allow for CH_3SH production. This experiment was semi-aerobic.

Following field sampling, the dissolved constituent data obtained from the same day as the dissolved gas samples was used to produce a new synthetic Cinder Pool water with a pH of approximately 4.5 (Table 1). This water was used for all following microcosm experiments, which were incubated for longer times and at varying temperatures. Based on observations from the autoclave experiments and knowledge of the conditions at the bottom of Cinder Pool, these experiments were carried out under anaerobic conditions only.

Anaerobic conditions were achieved by preparing all microcosms in an anaerobic chamber and removing all dissolved oxygen from the synthetic Cinder Pool water. In each experiment, the serum bottles were prepared in triplicates with either FeS, FeS_2, or cinder material collected from the pool, then capped, evacuated, and autoclaved. The FeS was powdered, and both the FeS_2 and cinder material were pulverized with a mortar and pestle to provide maximum reactive surface area. Once the bottles had been sterilized, 15 mL of sterile, synthetic Cinder Pool water was added to each bottle, and they were charged with a headspace of 50% H_2 and 50% CO_2 at a total pressure of 2.7 atm (Figure 8). The bottles were incubated for over a week in experiments 8, 9, and 10 (Table 2) at temperatures of 60, 80, and 100^{o}C respectively. Because the temperature at the bottom of Cinder Pool is at least 115.2^{o}C (the melting point of sulfur), there was initially an experiment planned for 120^{o}C as well. However, due to the operational temperature limit (~93^{o}C) of the butyl stoppers used to cap all serum bottles (ESI), an experiment at 120^{o}C was not performed.

One blank containing only synthetic cinder pool water (no solid material) and the imposed CO_2/H_2 headspace was also performed at each temperature. After initial concerns about these blanks that the butyl stoppers (more specifically, the curing agents used to prepare the rubber) may be introducing sulfur gases into experiments, a number of other blanks were performed (in triplicate) as well. Experiments 12 and 13 tested unused or "new" butyl stoppers with headspaces of either pure N_2 or the experimental mixture of H_2 and CO_2, and either no liquid, ultra-pure D.I. water, or the synthetic Cinder Pool water. All were incubated at 80^{o}C. After determining that SO_2 and CS_2 were

introduced to the bottles by "new" stoppers, experiment 14 compared serum bottles sealed with new stoppers to ones capped with previously used and visibly degraded "old" stoppers to determine if the curing agents could be removed after extended use and exposure to high heat and pressure. These bottles were not evacuated and had no headspace other than the air already present imposed; they were analyzed after being run through one 30 minute autoclave cycle. "Old" stoppers proved to be a viable tool for experiments where imposed CS_2 was not desirable.

Finally, a repeat of experiment 9 (experiment 15) was performed using degassed "old" stoppers to determine if the tested catalytic surfaces could also act as the sole source of sulfur and produce enough H_2S for subsequent formation of CS_2 and CH_3SH; 30 mL bottles were substituted for the 60 mL ones used previously due to availability. The chosen stoppers had already been used several times prior to the experiment, unlike the new ones used for experiments 8, 9, and 10, and they were further degassed by incubation in an 80^o oven for 2 weeks prior to use in experiment 15. No detectable sulfur gases were emitted by these stoppers.

2.5 GAS CHROMATOGRAPHY

Field gas samples were pressurized with N_2 to ~0.3 atm after collection to allow multiple analyses to be run from each sample. They were first analyzed for H_2 and CO using a TraceAnalytical RGA3 reduction gas analyzer connected to an SRI Model 202 four channel PeakSimple data system. Injection size for all analyses was 0.5 mL.

Both field and laboratory samples were analyzed for sulfur gases using an SRI Model 310 gas chromatograph (GC) and PeakSimple software. The GC measures the concentrations of different gases using both a flame ionization detector (FID) and a flame photometric detector (FPD). The gas sample is injected onto a column that separates individual gases for detection and measurement.

Two different columns were used during the course of analysis. During field analyses at the higher elevations of Yellowstone National Park, a Restek RT-XL sulfur column was used because of the greater separation between critical peaks and its dependability in field conditions. During laboratory analysis, for both the collected YNP samples and the microcosm experiments, a Restek MXT-1 column was used. While this column did present issues with peak separation between H_2S, COS, and SO_2, it was chosen for its greater sensitivity.

Gas concentrations were calibrated in PeakSimple using a sulfur gas standard containing 100 ppm each of H_2S, COS, CH_3SH, and $(CH_3)_2SH$ (ethanethiol, Eth-SH). Calibration standards for CS_2 and DMDS were made using a 1 L dilution bulb and 1 μL liquid injections, creating 400 ppm and 272 ppm standards respectively. A calibration curve for DMDS was created using Microsoft Excel for estimation at the lowest concentrations where the curve generated in PeakSimple was not satisfactory (Figure 9). The injection size for all analyses and calibrations was 0.5 mL.

During analyses, if a peak exceeded the detection limit, the visible portion of the peak was integrated and the value is reported as greater than that integrated value on bar graphs. If the ability to view a potential peak was inhibited by an exceptionally large

previous peak (e.g. an H_2S peak is so large that it extends past the retention time of CH_3SH), the area of the peak was estimated based on the visible portion of the peak and described as "coeluted" in graphs.

Gas concentrations were first converted to partial pressure in atmospheres and then to the equilibrium dissolved concentrations using Henry's Law. This required using the local air pressure at Norris Geyser basin (estimated to be approximately 0.72 atm) for field data and the imposed air pressure in the serum bottles for microcosm experiments. K_H constants were obtained from a compiled dataset and are presented in Table 3 (Sander 1999). These values were corrected for the various experimental temperatures using the Van't Hoff equation.

2.6 Environmental Scanning Electron Microscopy

Cinder structure was examined using a Phillips/FEI XL 30 Environmental Scanning Electron Microscope (ESEM), and elemental composition was characterized with Energy-Dispersive X-ray Spectroscopy (EDS). Sulfur material from the bottom of the pool and a whole cinder collected from the surface were analyzed to identify compositional changes the material may undergo as it floats to the surface, such as oxidation or sorption of other dissolved constituents in the pool. Elemental composition was analyzed at six sites on the pulverized bottom material and at 2 sites on the whole cinder piece.

Chapter 3: Results

3.1 Sulfur Gas Stability and Degradation

Results from the sulfur gas stability experiment are summarized in Figures 10-15. If a particular component was present at concentrations greater than the detection limit (over range), the corresponding point has been plotted at the top of the graph. It should be noted that, because of the overlap in retention time between COS and SO_2, there was no way to discern which gas was responsible for the peak although some of it is presumed to be SO_2 based on previous CH_3SH photooxidation research (Sie 1971). This peak has therefore been depicted as COS/SO_2. It was apparent that one or both of these gases increased with days elapsed, as the values measured from this peak were consistently higher over time in all bottles except air/water in dark. CS_2 had not been calibrated at the time of this experiment, so all values depicted on graphs are estimations based on post- calibrations and the relative response compared with other nearby peaks.

In all conditions, H_2S levels dropped over time while CS_2 emerged after a week and increased over the remainder of the experiment. Several bottles showed a minor increase in both Et-SH and Me-SH and occasionally H_2S at the one week measurement, but this is probably an artifact due to changing the carrier gas source over this period and should be disregarded. A tiny amount of DMDS (<1 ppm) was detected in all bottles from the beginning due to degradation within the standard gas that was used. This value remained fairly constant in dark bottles and increased in light bottles.

In both the dark and light dry air dilutions, CH_3SH and Eth-SH decreased over the first 24 hours and had dropped further by the 18 day mark. H_2S concentration in the light

bottle decreased by approximately twice as much as in the dark bottle. COS/SO_2 rose markedly in both bottles, but was over range after only a day in the light bottle, as opposed to a week in the dark bottle.

In the light N_2 diluted bottle, CH_3SH concentrations dropped consistently over the experimental period, while Eth-SH dropped after 24 hours and decreased again after 18 days as observed in the dry air dilutions. The dark N_2 bottle's CH_3SH concentration began over range and dropped significantly after the first 24 hours, and at the end of the 18 days it had declined to ~30 µmol/L. Eth-SH concentrations rose marginally over the first week but dropped below initial levels by the final measurement. H_2S decreased to similar final levels in both bottles, and the COS/SO_2 concentrations increased in both, albeit more quickly in the light exposed bottle.

In the light "normal" air dilution in presence of water bottle, both CH_3SH and Eth-SH dropped rapidly over the course of the experiment with no detectable amounts of either remaining in the bottle after 18 days. In the dark bottle, both gases dropped after 24 hours and decreased again to approximately 10 µmol/L between 7 and 18 days. After a week had elapsed, H_2S was no longer detected. The COS/SO_2 concentration remained above detection throughout the experiment in the light bottle and only peaked at a quantifiable level after 24 hours in the dark bottle. DMDS rose by the largest margin of the experiment in the light water bottle.

3.2 CINDER POOL GEOCHEMISTRY

Geochemical data for Cinder Pool from the USGS on the day of sampling are summarized in Table 1. Although generally one of the most chemically dynamic pools in the park (Xu et al. 2000), most unstable parameters and major dissolved constituent values remained fairly consistent across the three collections made that day. One exception to this is iron, which dropped from 0.14 mg/L to 0.08 mg/L before rising again to 0.13 mg/L during the 4.75 hours between the first and last samples' collection (Figure 16). Eh values recorded during this time fluctuated as well from 0.111 V to 0.062 V then back up to 0.080 V. Bromide and silica showed a similar trend, although not as dramatic in terms of percent change, while potassium and zinc both rose in the second sample and dropped again in the third. The pH dropped from 4.38 to 4.27 during this time and the recorded temperature near the surface was 90.6^{o}C.

In-situ GC analyses of Cinder Pool's dissolved gases were not sensitive enough to quantify the presence of alkyl-thiols, but note that a small COS peak was detected at 3 m depth, and potential COS and CH_3SH peaks were observed at 17 m depth, although these were not defined enough to confidently claim detection (Figures 17 and 18). Laboratory analyses of field samples are summarized in Table 4. In addition to values for Cinder Pool, gas concentrations for a pool with a black, coated bottom near Cinder Pool have been included, since CH_3SH was detected there as well. All Cinder Pool samples contained CS_2, but at the time of analysis the lab did not have the ability to calibrate the peak magnitudes. CS_2 values are therefore estimated for the purpose of showing relative abundance. While all samples had H_2S concentrations above the detection limit (all

greater than ~24 μmol/L with individual variability) on the gas chromatograph, colleagues from the USGS found concentrations between 49.9 and 73.4 μmol/L by titration. COS was detected in all of the field sample bottles, from both Cinder Pool and the nearby pool. Because both COS and CS_2 increased in bottles over time during the stability experiments, the values given for field samples are likely higher than what was originally present in the water and have not been displayed as a dissolved concentration from the pool. Figure 19 displays gas concentration vs. depth for all samples in Cinder Pool. In general the highest concentrations of gases were recorded at the bottom of Cinder Pool, although the highest overall CH_3SH concentration was detected in the nearby pool. CH_3SH detection does not appear to correlate with the presence of any other gases.

Cinder material composition determined by EDS elemental analysis is presented in Table 5 with X-ray spectrum data provided in Figures 20-27. Analyses 1-6 were performed on pulverized material from the bottom of the pool while analyses 7 and 8 were performed on a whole cinder collected from the surface of the pool. Bottom material was predominantly elemental sulfur with small amounts of iron and aluminum detected as well. Contents of the whole cinder were significantly more heterogeneous. While it too was dominated by elemental sulfur, it also contained iron, aluminum, silicon, titanium, potassium, and significant oxygen. Two ESEM images depicting the structure of intact cinders are provided as well (Figures 29 and 30).

3.3 POOL MICROCOSMS

Results of microcosm experiments are reported as dissolved gas concentration in μmol/L and summarized in Tables 6 through 10, and all concentrations were normalized to 1 gram of the provided solid for graphs. Cinder bottles consistently yielded the highest levels of both CH_3SH and CS_2, and higher temperatures also facilitated sulfur gas production.

3.3.1 Elemental Sulfur

Microcosms with S^0 as the sole sulfur source in a semi-aerobic environment yielded only H_2S as a byproduct. This was the result when using both synthetic Cinder Pool water and dilute HCl (Figure 31). H_2S was detected at 4.24, 8.17, and 5.35 μmol/L in the synthetic Cinder Pool water bottles, and at 8.21, 9.93, and 9.68 μmol/L in the dilute HCl bottles. As the values obtained in both scenarios were similar, only the synthetic Cinder Pool water was used when this experiment was repeated anaerobically. In the anaerobic microcosms (which used new stoppers), concentrations of H_2S were over detection limits even with low sensitivity settings on the GC. CS_2 was detected and estimated to be below 0.25 μmol/L in all four bottles. Both the anaerobic and semi-aerobic gas concentrations in synthetic Cinder Pool water have been compared in Figure 32.

3.3.2 Ferrous Sulfide

Semi-aerobic microcosms that used FeS as the solid and contained a headspace of CO_2 in general yielded substantial amounts of H_2S and CS_2, and low but detectable quantities of CH_3SH (Table 7 and Figure 33). Bottles 1-1 and 1-2 contained dilute HCl, and 1-2 was the only one that did not contain detectable CH_3SH whereas 1-1 produced 0.005 µmol/L, the highest amount measured in this experiment. Bottles 3-1 and 3-2, containing synthetic Cinder Pool water, both yielded CH_3SH concentrations of 0.001 µmol/L or less. H_2S concentrations ranged from 0.64 to 0.17 µmol/L, COS concentrations were all ~0.02 µmol/L, and CS_2 ranged from approximately 0.03 to 0.08 µmol/L. Whether stoppers used were old or new was not recorded at the time of this experiment.

The triplicates of FeS bottles in experiments 8, 9, and 10 were numbered 1 to 3. At 60°C, H_2S, CH_3SH, CS_2, and DMDS were detected in all three bottles (Figure 34). CH_3SH was consistently measured at <0.5 µmol/L in all bottles, and DMDS values were also consistent at approximately 2 µmol/L. Both H_2S and CS_2 were more variable among the 60° triplicates. At 80°C, H_2S, CH_3SH, CS_2, and DMDS were once again identified in all three bottles, with Eth-SH also measured in each bottle (Figure 35). H_2S peaks were over range (greater than 6.3 µmol/L) in all bottles, and CH_3SH levels were much higher than those recorded at 60°C, with the concentration in 9-2 being above the detection limit at greater than 7.2 µmol/L. Values for CS_2 and DMDS were substantially lower than at 60°C: < 0.1 µmol/L for CS_2 and < 0.4 µmol/L for DMDS. All three bottles incubated at 100°C contained 2 to 4 µmol/L of CH_3SH and H_2S concentrations > 30 µmol/L, (Figure

36). Less than 0.02 μmol/L of Eth-SH was measured in each bottle. No CS_2 or DMDS was detected in any of the 100°C triplicates.

3.3.3 Pyrite

Triplicates containing pyrite were labeled 4 through 6 across the three experiments. The gases identified at 60°C were inconsistent among the three bottles and the only gas detected in all of them was CS_2, and although it was present in 8-6 the peak was too small to confidently estimate a concentration (Figure 37). H_2S exceeded detection limits (> 8.26 μmol/L) in 8-5 but was not detected at all in the other two bottles. CH_3SH formed in 8-5 and 8-6 at concentrations of 0.92 and 0.28 μmol/L respectively, and an Eth-SH peak was observed in 8-6. At 80°C, all three bottles contained H_2S, CH_3SH, CS_2, and DMDS with H_2S concentrations above the detection limit in all samples (Figure 38). CH_3SH concentrations were much higher than those at 60°C, with the peak in 9-5 above the detection limit, or greater than 8 μmol/L. CS_2 and DMDS were more consistent than in experiment 8, with the lowest concentrations of each measured in 9-4, the bottle that also contained the lowest concentration of CH_3SH. At 100°C, bottles containing pyrite all contained quantifiable amounts of H_2S: 16.19, 14.55, and 13.22 μmol/L in 10-4, 10-5, and 10-6 respectively. In Figure 39, these values have been normalized and provided numerically where the H_2S bars have been cut off to allow more detailed viewing of less abundant gases. It should be noted that while the H_2S peaks themselves were not over range, the value obtained in ppm was outside of the calibrated range, and the provided dissolved concentration is merely an estimate based on those

values. All the bottles contained measurable amounts of CH_3SH, Eth-SH, CS_2, and DMDS. CH_3SH was measured in each bottle at 5.12, 4.87, and 3.46 µmol/L; Eth-SH at 0.033, 0.032, and 0.044 µmol/L; and DMDS at 0.018, 0.351, and 0.527 µmol/L in 10-4, 10-5, and 10-6 respectively. CS_2 ranged approximately from 0.02 to 0.06 µmol/L.

3.3.4 Cinder material

Triplicates containing cinder material were labeled 7 through 9 at all three experimental temperatures. At 60°C, overall estimated CS_2 concentrations were higher in the cinder bottles than in either the FeS or the FeS_2 bottles with up to ~0.6 µmol/L (Figure 40). DMDS was detected in small amounts in all three bottles as well, but CH_3SH was only detected in 8-9 at 0.28 µmol/L. H_2S was comparatively low in 8-7 at 1.2 µmol/L and exceeded the detection limit in both of the other two bottles at > 7 µmol/L and >10 µmol/L. At 80°C CH_3SH was estimated (due to coelution) to be ~3.4 µmol/L in 9-7 and < 1 µmol/L in 9-9, but was completely coeluted with H_2S in 9-8 making an estimation impossible. H_2S and CS_2 exceeded detection limits in all three of the bottles, and were at least an order of magnitude greater in abundance in the cinder bottles than in the FeS or FeS_2 bottles at 80°C (Figure 41). DMDS was only detected in 9-7 at 2.25 µmol/L. Eth-SH was detected in all three bottles, but was fairly distorted due to severe coelution; estimates range from 0.28 to 6.27 µmol/L. At 100°C, H_2S, CH_3SH, and CS_2 were detected in all three cinder microcosms (Figure 42). H_2S levels were the highest seen in any of the experiments, exceeding detection limits at > 70 µmol/L. Estimated CS_2 concentrations were from 3-4 µmol/L. DMDS was detected at 0.18

μmol/L in 10-7, and Eth-SH was measured at 0.637 μmol/L in 10-9. CH_3SH was measured at 0.340, 0.748, and 2.008 μmol/L.

3.3.5 Blanks and Butyl Stopper Experiments

Gases found in the blanks from experiments 8, 9, and 10 (performed at 60, 80, and 100°C) are shown in Figure 43. CS_2 was detected in all of the blanks, and was above the detection limit at 80 and 100°C. Small peaks presumed to be COS were observed at 80 and 100°C, estimated at 0.12 and 0.03 μmol/L respectively.

Analysis of the headspace above the synthetic Cinder Pool water in its storage vessel indicated these gases were not generated by the media, so it was inferred that the butyl stoppers may be the source. Research about the specific stoppers used in these experiments, including discussion with the supplier, yielded no explanation. However, butyl rubber in general, like other unsaturated elastomers, is commonly cured in sulfur to minimize degradation (eFunda 2013). Specifically, dry SO_2 is used in a number of applications.

Experiments 12 and 13 tested unused stoppers under a variety of conditions (Table 11). Most notably, in the dry bottles with only an imposed headspace of either CO_2/H_2 or N_2, a CS_2 peak and a presumable SO_2 peak were observed in all triplicates. When liquid of any kind was present, only CS_2 was observed in the bottles, likely because of the large K_H constant for SO_2 in water which results in rapid dissolution into the aqueous phase (Table 3).

Experiment 14 compared new stoppers to previously used ones after one cycle through the autoclave with no special headspace imposed (Table 12). All new-stoppered bottles contained both SO_2 and CS_2 while only one of the old stoppered bottles did, and the peaks in that bottle were observed to be much smaller than those from new stoppers.

Experiment 15, which repeated 9-1: 9-10 at 80°C with old and additionally degassed stoppers, did not repeat the results from experiment 9 (Table 13 and Figures 44-46). The gas distribution observed in 15-7: 15-9 was remarkably similar to 9-7: 9-9 in that their large H_2S peaks coeluted with several of the proceeding gases, and all three bottles produced CH_3SH, Eth-SH, and CS_2. The FeS and FeS_2 bottles, however, only produced low concentrations of H_2S. The blank bottle with only synthetic Cinder Pool water contained no sulfur gases.

Chapter 4: Discussion

4.1 Sulfur Gas Stability and Degradation

Sulfur gas stability experiments suggest that both photolysis and moisture exposure accelerate sample degradation. Of the bottles exposed to sunlight, CH_3SH constantly decreased over the 18 day period in both the N_2 diluted and air diluted in presence of water samples, while the dry air diluted sample increased slightly after a week (experimental artifact) but still decreased by over half after 18 days.

Photo dissociation is a common chemical process where a photon absorbed by a molecule has more energy than what is needed for bond dissociation, causing the molecule to break apart (Sturm 1969). In the case of CH_3SH, photolysis would follow reactions (8-10).

$$CH_3SH + h\nu \rightarrow CH_3S\bullet + H\bullet \quad (8)$$

$$CH_3SH + H\bullet \rightarrow CH_3S\bullet + H_2 \quad (9)$$

$$CH_3S\bullet + CH_3S\bullet \rightarrow CH_3SSCH_3 \quad (10)$$

where further reactions create byproducts such as methane, ethane, and H_2S but are not as well understood (Oae 1992). This explains why the final CH_3SH concentration in each of the dark bottles was higher than in their sun-exposed counterparts. The photo dissociation effect seems to be enhanced in the bottle containing synthetic Cinder Pool water, as it had no detectable CH_3SH remaining after 18 days elapsed. Reactions with hydroxyl radicals ($OH\bullet$) are most likely responsible for the additional decrease of CH_3SH concentration in the presence of water. Hydroxyl radicals can form from a number of

possible processes (Stumm and Morgan 1996) and would react with CH_3SH to form $CH_3S\bullet$ and H_2O (reaction 11).

$$CH_3SH + OH\bullet \rightarrow CH_3S\bullet + H_2O \quad (11)$$

These findings indicate that the CH_3SH detected in the field samples did not form in the bottles as a result of degradation reactions. The environment inside field samples most closely resembled the stability scenarios diluted with air in the presence of water. Because the samples were exposed to sunlight during collection only until they could be placed in the storage cooler (probably from 1 to 4 hours exposure depending on collection time), and they contained some unavoidable moisture, the reported values from Cinder Pool are considered minimums.

These experiments also show that through some means, COS and/or SO_2 are degradation products of H_2S, CH_3SH, and Eth-SH. A COS/SO_2 peak eluted for each of the field samples that was analyzed in the laboratory. Because these values were at least in part a result of degradation, they were disregarded.

4.2 CINDER POOL GEOCHEMISTRY

4.2.1 Cinder Composition and Structure

The molten sulfur layer at the bottom of the pool is a heterogeneous mixture rather than a uniform substance. The amount and even the presence of aluminum and iron was unpredictable between sampling locations, suggesting a highly inconsistent composition throughout the subaqueous layer. There may be even more variability in composition at other locations on the floor of the pool than the one sampled.

Furthermore, it is not known how much deeper below the sulfur/water interface the molten material continues, or what the water content is within the molten material, and there may be variations with depth below that point as well.

The floating cinders contained various elements not found in the bottom material and typically associated with clays, suggesting that the cinders interact with dissolved constituents in the water as they float to the surface. The significant presence of oxygen in the surface cinders implies that they either incorporated water into the structure, or they were exposed to the air before collection, as the shallowest depths of the pool are a more oxidizing environment than the bottom. The degree of variability between these two sites is also indicative of heterogeneous composition in the cinders.

Pulverized cinder material that was used in microcosm experiments was autoclaved inside the bottles during sterilization. The high temperatures necessary for sterilization exceed the melting point of elemental sulfur (115.2^{o}C), which makes up the majority of the cinders' composition. This caused preferential melting of the sulfur, and a degree of separation from the other minor compounds in the material. Yellow color was observed where it is not in intact cinders or the collected subaqueous material (Figure 47). This separation may expose more surface area of the minor constituents such as FeS_2, allowing more opportunity for their participation in reactions.

Structure was impossible to determine from the bottom material because of disorder inflicted while grinding with a mortar and pestle. These individual particles did not appear especially unique and were on the order of a few hundred μm in diameter (Figure 28). Some smaller particles of <10 μm are apparent as well as some small pore

spaces. However, two ESEM images taken of a whole cinder piece (Figures 29 and 30) depict a highly vesicular texture with visible pores ranging in scale from <20 μm to a few hundred micrometers in diameter. Figure 30 in particular shows a fracture connecting several of these pores. These small, enclosed spaces may serve to concentrate key gases by forcing reactions to occur in proximity to the catalytic surface.

4.2.2 Water chemistry

Measured Eh and dissolved iron in the pool are correlated (Figure 16). Eh measured in the field is indicative of the potential for the dominant redox couple that is electroactive on the platinum electrode surface (Stumm and Morgan 1996) which is typically the Fe^{2+}/Fe^{3+} couple. The observed correlation between Eh and dissolved iron in Cinder Pool suggests that Fe^{2+}/Fe^{3+} is the dominant redox couple. As iron-mediated reactions are key to the hypothesized processes occurring in the pool, this finding was encouraging for the planned structure of laboratory experiments.

The environment in Cinder Pool is highly dynamic, and a clear trend in dissolved gas concentrations with depth was not apparent. The highest concentrations of most gases were found at 18 m depth—approximately at the sulfur/water interface, where some of the bottom material was sucked into the sampling tube—but concentrations within the water column varied greatly. The greater abundance of all gases at the deepest sampling depth is likely a result of the higher temperature (at least 115.2^{o}C) and proximity to the source of dissolved gases, and concentrations are likely higher within the sulfur layer due to its higher viscosity which can trap gases more easily.

Because the production of CH_3SH is probably H_2 limited in natural environments (Schulte and Rogers 2004), the higher concentrations of H_2 at the sulfur/water interface (Figure 19) support the hypothesis that the cinder material is a reactive site for the key reactions for forming CH_3SH and beyond. Furthermore, because the pores of the cinders that float to the surface trap the gases found in this subaqueous material, they represent another possible refuge for the procession of surface metabolism reactions.

4.3 EXPERIMENTAL ARTIFACT

The butyl rubber septa used in the microcosm experiments, and which are used almost universally worldwide for anaerobic microbial microcosm experiments, introduced an unforeseen and previously undocumented artifact. The rubber used in the manufacture of the septa is sulfur cured, either with SO_2 or CS_2, and when new stoppers are heated they will outgas either or both of these compounds for a period of time. This was clearly a source of both CS_2 and SO_2 in the experimental microcosms, although this artifact was not detected in the field sample bottles that were maintained at low temperature.

SO_2 is detected in the headspace gas only with dry bottles, and is differentiated from the co-eluting COS peak by its absence in bottles containing water, which is indicative of a large Henry's partitioning constant (K_H) value. The K_H of SO_2 at STP is 1.4, so it will preferentially partition into aqueous phase from the headspace gas phase (Sander 1999). Conversely, the K_H of COS is 0.022, so it would still be expected to partition into the headspace gas phase, making it detectable where SO_2 is not.

While originally unintended, the introduction of large CS_2 concentrations to the microcosms supports the argument that the iron sulfide minerals contained in the cinder material act a catalytic surface, and that the basic mechanism for CH_3SH synthesis uses CS_2 as an intermediate. The critical reaction requiring surface catalysis is the hydrogenation of CS_2 to form CH_3SH and H_2S.

$$CS_2 + 3H_2 \rightarrow CH_3SH + H_2S \quad (6b)$$

All microcosm experiments were pressurized with a PH_2 of ~1.35 atm, meaning that the addition of relatively high concentrations of CS_2 into the blank bottles provided all of the reactants needed for CH_3SH production in the blank bottles, yet none of the blanks (which did not contain a catalytic surface) generated any CH_3SH. The experimental bottles, however, contained a catalytic surface (cinder material, FeS, or pyrite) and at the temperatures found in Cinder Pool, all three surfaces catalyzed the hydrogenation of CS_2 to CH_3SH (Figures 36, 39, 42). Recent research suggests that this reaction mechanism, in the presence of a transition metal sulfide catalyst, is a much more significant pathway for production of CH_3SH than the generally accepted hydrogenation of COS (Gutiérrez et al. 2011).

4.4 Reactive and Catalytic Surfaces

All three iron sulfide solids tested in this study effectively catalyzed reaction (6b) when a high concentration of CS_2 (from the stoppers) was imposed on the microcosms. However, FeS and FeS_2 bottles produced CH_3SH only when CS_2 was added to the

bottles, and generated only small amounts of H_2S without the addition of CS_2 (experiment 15). I drew a couple of conclusions from this:

1) FeS and FeS_2 are both capable of catalyzing the hydrogenation of CS_2 into CH_3SH if enough CS_2 is present.
2) In an analog Cinder Pool environment, FeS and FeS_2 alone are not capable of producing enough H_2S for the subsequent generation of CS_2 and CH_3SH.

This second presumption differs from other studies, which found that both CS_2 and CH_3SH were produced using only FeS as a reactive surface (Heinen and Lauwers 1996). However, those experiments used pure HCl to generate enough H_2S (reaction 4) for the subsequent reactions or they imposed H_2S directly, while my experiments depended on a solution with a higher pH of ~4.5 for H_2S generation. The weaker acid used in an effort to replicate Cinder Pool's conditions in this study would have limited the amount of H_2S formed from reaction (4). However, pure FeS as a reactive surface for reactions (4-6) may be viable in more acidic hydrothermal features.

In contrast, bottles containing pulverized cinders consistently generated the highest concentrations of H_2S, greatly exceeding the GC detection limits and perturbing the responses of the three subsequent components (COS/SO_2, CH_3SH, and occasionally Eth-SH). More notably, cinder bottles produced measurable CS_2 and CH_3SH even when no additional CS_2 was introduced by the stoppers. These findings were consistent with the gases detected in field samples. Two conclusions can be made from these results as well:

1) Something about the cinders causes them to produce much larger concentrations of H_2S than either of the purely iron sulfide compounds.
2) Something in or on the cinders catalyzes CH_3SH generation (reaction 6b).

The large quantities of H_2S produced by the cinders must be sourced from the elemental sulfur of which they are mainly composed, presumably by the reaction of S^0 with free hydrogen in the water. Even in the short (12 hours) experiments, substantially larger concentrations of H_2S formed in the presence of S^0 than what was observed in FeS bottles, and in the fully anaerobic S^0 bottles CS_2 was detected as well (Figures 32 and 33). This shows that S^0 in water is a good source of H_2S, and that under conditions found in Cinder Pool the formation of CS_2 (reaction 6a) is spontaneous whereas the formation of CH_3SH (reaction 6b) requires a catalyst.

It is clear from the experiments using elemental sulfur that it does not act as the catalyst for CH_3SH generation. It is also clear from the FeS and FeS_2 experiments that they can serve as a catalyst in these conditions as long as there is another source of CS_2. This is also supported by recent research (Gutiérrez et al. 2011; Rushdi and Simoneit 2005). Cinders contain small amounts of iron sulfide minerals, and because they also contain so much S^0, they produce enough H_2S and subsequently CS_2 to fuel the CH_3SH generating reaction, catalyzed by those iron sulfide compounds. Because the cinder material contains both S^0 and iron sulfide compounds, it can virtually serve as a CH_3SH factory if the right dissolved gases are present, as in Cinder Pool. Furthermore, thousands of floating cinders in addition to the molten cinder material at the bottom of the pool provide a large surface area on which these reactions can proceed.

Chapter 5: Implications for the Origin of Life

Methanethiol has now been identified in Cinder Pool, and the water and dissolved gas composition are all consistent with an abiotic synthesis pathway. I have also replicated the Cinder Pool conditions in the laboratory, and have been able to synthesize CH_3SH and other important sulfur gas compounds abiogenically in this environment. An important question however, is whether the CH_3SH in Cinder Pool is truly abiotic in origin, or if it is part of a microbial synthesis pathway.

Methanethiol is a byproduct of algae degradation and microbial sulfate reduction (Lomans et al. 1997). It is also a substrate for methanogens, and aerobic methylotrophs. Currently the only microbial population identified in Cinder Pool is *Aquificales Hydrogenobaculum,* an organism that uses the reductive citric acid or reverse Krebs cycle (Hügler et al. 2007; Reysenbach et al. 2009). This metabolism is the extant version of the proposed surface metabolism (Wächtershäuser 1990b; Wächtershäuser 1988b), and it oxidizes sulfide compounds such as CH_3SH, as well as H_2. This makes it extremely unlikely that CH_3SH detected in the pool is of biogenic origin, and much more likely that the microbial populations could be utilizing it as an energy source.

The 'cinders' in the pool have an intriguing structure and composition that has implications for the theorized prebiotic synthesis of organic biomolecules. Previous research has suggested that permeable membranes may have formed along redox boundaries between alkaline submarine hot spring discharge and an acidic Hadean ocean (Martin and Russell 2007; Russell and Hall 1997). These membranes could have

functioned as the first primitive "cellular membrane," serving to contain reactants and mobilize them away from the hotter environment in the immediate vicinity of the vent. Cinders—large bubbles themselves—contain numerous enclosed spaces of the same size proposed by those previous studies, many on the order of 10 μm (Figures 22 and 23). Furthermore, cinders provide this structure in an environment that doesn't necessitate the alkaline solution proposed by others, allowing the reactions to be facilitated in more than one type of hydrothermal environment. While the membrane proposed by Russell and Hall is purely an "iron monosulphide bubble," or FeS, and the cinders are composed largely of elemental sulfur with minor iron sulfide components, the similarity between the two structures and their potential function to enclose and catalyze the first surface metabolic reactions is worthy of note. The composition of the cinders in an Archaean 'Cinder Pool' with a more reducing environment would have had a much higher concentration of ferrous iron and potentially a greater abundance of the reactive catalytic surface, and therefore more reaction potential.

One advantage of the original theory proposed by Wächtershäuser was that high concentrations of reactants are not necessary in solution because the pyrite surface would act to concentrate them and facilitate their reaction (Wächtershäuser 1994; Wächtershäuser 1990b; Wächtershäuser 1988b). The low concentrations of CH_3SH identified in Cinder Pool and the nearby pool are not considered a limitation for their potential participation in the proposed surface metabolism. Samples from Cinder Pool were collected from the middle of the pool and should not be expected to reveal microscopically thin layers of concentrated key reactants on mineral surfaces.

While past research has focused on interactions between FeS and acidic water as the source for all reactants leading to CH_3SH production (Heinen and Lauwers 1996; Schulte and Rogers 2004), little has been said about other sources of H_2S in these environments because it is generally ubiquitous. However, among samples run from other features in the park, Cinder Pool revealed the highest H_2S concentrations, even among other Norris Geyser Basin features. This increased sulfide is presumably sourced from the molten sulfur layer at the bottom reacting with molecular hydrogen. While not really addressed by others, it seems like environments that contain both catalytic minerals and elemental sulfur as Cinder Pool does are an ideal setting for these reactions.

One assertion of a hyperthermophilic chemoautotrophic origin of life is that it would not require a deeply reducing atmosphere or limit the location for reactions to a water/air interface (Wächtershäuser 1988b). The required processes could occur anywhere the chemical and mineralogical conditions are met. Abiotic CH_3SH production was originally hypothesized to occur only at acidic mid-ocean ridge vents, and while findings by others suggest this possibility (Dias et al. 2010; Heinen and Lauwers 1996; Schulte and Rogers 2004; Wächtershäuser 1988b), it has now been documented in a terrestrial hydrothermal environment. Other potential locations for this process are numerous, and the so-called "white smoker" vents that issue alkaline rather than acidic solutions in places such as Lost City only represent one possibility (Huber and Wächtershäuser 1997; Russell and Hall 1997). Even beyond the origin of life on earth, processes at hydrothermal vents have been implicated as a source of possible life in the theorized subsurface oceans of Europa (NASA Headline News 2001).

Tables

USGS ID	11WA174	11WA175	11WA176
Time Collected	10:30:00 AM	1:20:00 PM	3:15:00 PM
Filtration µm	0.1	0.1	0.1
pH field	4.38	4.37	4.27
pH, Lab	4.26	4.24	4.25
SC µS	2160	---	---
SC, Lab	2350	2360	2350
Temp C	90.6	---	---
DOC, mg/L	0.9	1.1	0.8
density	0.99936	0.99940	0.99934
Eh, V	0.111	0.062	0.080

Anions			
USGS ID	11WA174	11WA175	11WA176
F	7.9	8.2	8.1
Cl	598	603	598
Br	2.5	1.7	2.3
NO3	<0.05	<0.05	<0.05
SO4	54.4	53	57.1
H2S	1.7		2.5

Cations			
USGS ID	11WA174	11WA175	11WA176
Al	0.770	0.766	0.768
As	2.54	2.51	2.55
B	9.32	9.15	9.30
Ba	0.020	0.020	0.020
Be	0.0003	0.0002	0.0003
Ca	5.47	5.45	5.45
Cd	<0.002	<0.002	<0.002
Co	<0.002	<0.002	<0.002
Cr	<0.002	<0.002	<0.002
Cu	<0.001	<0.001	<0.001
Fe(T)	0.014	0.008	0.013
Fe(II)	0.014	0.008	0.013
K	53.0	56.8	51.7
Li	3.68	4.54	4.64
Mg	0.023	0.023	0.024
Mn	0.003	0.003	0.003
Mo	0.112	0.109	0.108
Na	382	372	377
Ni	<0.004	<0.004	<0.004
P	<0.05	<0.05	<0.05
Pb	0.03	<0.02	0.02
Rb	0	0	0
Sb	<0.03	0.03	<0.03
Se	<0.06	<0.06	<0.06
SiO2	349	333	342
Sr	0.018	0.018	0.018
V	<0.002	<0.002	<0.002
Zn	0.002	0.007	0.002

Table 1: Cinder Pool unstable parameters and dissolved constituents collected by members of the USGS who collaborated with this work. Courtesy of D. Kirk Nordstrom, R. Blaine McCleskey, Kate M. Campbell, James W. Ball, and Randall Chiu.

	Experiment 8	Experiment 9	Experiment 10
Variable	60°C	80°C	100°C
FeS	8-1	9-1	10-1
	8-2	9-2	10-2
	8-3	9-3	10-3
FeS_2	8-4	9-4	10-4
	8-5	9-5	10-5
	8-6	9-6	10-6
Cinders	8-7	9-7	10-7
	8-8	9-8	10-8
	8-9	9-9	10-9
Water Blank	8-10	9-10	10-10
All experiments contained a 50/50 headspace of Hydrogen and Carbon Dioxide at ~2.7 atm			

Table 2: Array of variables in Experiments 8, 9, and 10

Henry's Constants at 25°C				
Gas	KH	ΔH/R	Source	Type of source
H_2	0.00078	500	Lide and Frederikse 1995	Literature Review
CO	0.00099	1300	Lide and Frederikse 1995	Literature Review
SO_2	1.4	2900	Lide and Frederikse 1995	Literature Review
H_2S	0.087	2100	De Bruyn et al. 1995	Measured Value
COS	0.022	2100	De Bruyn et al. 1995	Measured Value
CH_3SH	0.2	2800	De Bruyn et al. 1995	Measured Value
Eth-SH	0.28	3800	Przyjazny et al. 1983	Measured Value
CS_2	0.055	2800	De Bruyn et al. 1995	Measured Value
DMS	0.48	3100	De Bruyn et al. 1996	Measured Value
DMDS	0.96	4000	Przyjazny et al. 1983	Measured Value

Table 3: Table of Henry's Law constants used in this study for determining dissolved gas concentrations. All of these values were obtained from Sander 1999.

Sample I.D.		YNP11-006	YNP11-010	YNP11-012	YNP11-014	YNP11-015	YNP11-016	YNP11-007
Site Description		Cinder Pool						Pool near CP
Depth		-2 m	-1 m	-3 m	-10 m	-18 m	-17 m	-2 m
Headspace concentration in ppm	H_2	69.72	86.86	97.69	81.35	136.9	72.05	28.94
	CO	37.57	34.19	33.01	18.6	51.65	48.15	13.26
	H_2S	>26.16	>26.74	>26.28	>28.79	>33.47	>24.27	>23.96
	COS	2.52	2.21	1.54	4.19	9.62	1.46	0.51
	CH_3SH	0	0	0	**0.02**	0	0	**0.165**
	CS_2	0.05	0.01	0.02	0.06	0.09	0.01	0
Dissolved concentration in µmol/L	H_2	0.0289	0.0360	0.0405	0.0338	0.0568	0.0299	0.0120
	CO	0.0122	0.0111	0.0107	0.0060	0.0168	0.0156	0.0043
	H_2S	Determined by titration: between 49.9 and 73.4 µmol/L						>0.42
	COS	Potentially partially a result of degradation within bottle, not converted to dissolved concentrations						
	CH_3SH	0	0	0	**0.0005**	0.0000	0	**0.0044**
	CS_2	Potentially partially a result of degradation within bottle, not converted to dissolved concentrations						

Table 4: Measured concentrations of dissolved gases in natural hot spring waters as determined via gas chromatography. Hydrogen Sulfide was over the detection limit for all samples and thus impossible to accurately quantify at sensitivities needed for detecting alkyl thiols, but was determined in the field by titration. Headspace partial pressures in the bubble have been converted to dissolved concentrations of each gas reported in µmol/L. Samples containing methanethiol have been presented in bold.

Site	Material	Element by weight percent						
		S	Fe	Al	O_2	Si	Ti	K
1	Ground Cinder bit 1	37.86	0	0	0	0	0	0
2	Ground Cinder bit 1	48.26	0.30	0	0	0	0	0
3	Ground Cinder bit 2	36.02	0.74	0.42	0	0	0	0
4	Ground Cinder bit 2	49.20	1.60	0.45	0	0	0	0
5	Ground Cinder bit 2	55.32	0.31	0.44	0	0	0	0
6	Ground Cinder bit 3	54.23	0.38	0.31	0	0	0	0
7	Whole Cinder	37.57	0.88	0.40	10.22	1.11	0.11	0
8	Whole Cinder	4.69	0.15	0.48	7.97	3.50	0	0.21

Table 5: Weight percent of detected elements in cinder materials as determined by EDS

Sample I.D.	Contents	Temp (°C)	head space (ppm)		raw (µmol/L)		norm (µmol/L)	
			H_2S	CS_2	H_2S	CS_2	H_2S	CS_2
CP-S: 4	Sulfur, Synthetic Cinder Pool Water, Semi Aerobic	121	133.00	0	4.24	0	1.04	0
CP-S: 5			256.13	0	8.17	0	1.90	0
CP-S: 6			167.77	0	5.35	0	1.30	0
HCl-S: 4	Sulfur, Diluted HCl, Semi Aerobic	121	257.44	0	8.21	0	1.95	0
HCl-S: 5			311.11	0	9.92	0	2.26	0
HCl-S: 6			303.39	0	9.68	0	2.30	0
CP-S: 7	Sulfur, Synthetic Cinder Pool Water, Anaerobic	121	>537	20.00	>17.13	0.23	>4.28	0.06
CP-S: 8			>544.80	16.00	>17.38	0.18	>4.34	0.05
CP-S: 9			>532.30	15.50	>16.98	0.18	>4.24	0.04
CP-S: 10			>551.40	16.00	>17.59	0.18	>4.40	0.05

Table 6: Gas concentrations from elemental sulfur experiments. Yellow column is normalized to 1 gram of solid.

Sample I.D.		FeS: 1-1	FeS: 1-2	FeS: 3-1	FeS: 3-2
Contents (CO2 only, anaerobic)		FeS, Dilute HCl		FeS, Synthetic Cinder Pool Water	
Temperature (^{o}C)		121			
head space	H2S (ppm)	30.224	20.356	8.550	7.867
	COS (ppm)	4.000	3.000	3.500	3.200
	CH3SH (ppm)	0.170	0.000	0.009	0.035
	CS2 (ppm)	4.000	5.000	10.000	5.000
raw	H2S (µmol/L)	0.642	0.433	0.182	0.167
	COS (µmol/L)	0.021	0.016	0.019	0.017
	CH3SH (µmol/L)	0.005	0.000	0.000	0.001
	CS2 (µmol/L)	0.030	0.038	0.076	0.038
norm	H2S (µmol/L)	6.328	3.761	1.285	1.328
	COS (µmol/L)	0.212	0.140	0.133	0.137
	CH3SH (µmol/L)	0.046	0.000	0.002	0.008
	CS2 (µmol/L)	0.299	0.330	0.536	0.301

Table 7: Gas concentrations from FeS overnight experiments containing no imposed H_2. Yellow rows are normalized to 1 gram of solid. Experiments at this time did not differentiate between "old" or "new" stoppers, and therefore it is not known if or how much CS_2 was introduced to this experiment.

		FeS			FeS2			Cinders			Blank
		8-1	8-2	8-3	8-4	8-5	8-6	8-7	8-8	8-9	8-10
Raw (µmol/L)	H2S	1.84	1.27	6.43	0.00	**>8.26**	0.00	1.20	**>7.49**	**>10.78**	0.00
	COS	0.00	0.00	0.00	0.00	0.00	0.04	0.00	0.00	0.00	0.00
	CH3SH	0.32	0.28	0.58	0.00	0.92	0.28	0.00	0.00	0.28	0.00
	Eth-SH	0.00	0.00	0.00	0.00	0.16	0.00	0.00	0.00	0.00	0.00
	DMS	0.00	0.00	0.00	0.00	0.00	1.63	0.00	0.00	0.00	0.00
	CS2	0.20	0.23	0.03	0.28	0.02	present	0.56	0.22	0.49	0.27
	DMDS	1.94	1.89	2.01	1.36	2.00	0.00	0.64	1.27	1.08	0.00
Normalized (µmol/L)	H2S	1.03	0.69	2.94	0.00	**>12.40**	0.00	1.93	**>18.63**	**>13.89**	NA
	COS	0.00	0.00	0.00	0.00	0.00	0.05	0.00	0.00	0.00	NA
	CH3SH	0.18	0.15	0.26	0.00	1.38	0.37	0.00	0.00	0.36	NA
	Eth-SH	0.00	0.00	0.00	0.00	0.24	0.00	0.00	0.00	0.00	NA
	DMS	0.00	0.00	0.00	0.00	0.00	2.16	0.00	0.00	0.00	NA
	CS2	0.11	0.13	0.02	0.25	0.03	present	0.90	0.55	0.63	NA
	DMDS	1.08	1.03	0.92	1.20	3.00	0.00	1.03	3.17	1.40	NA

Table 8: Results from Experiment 8. Both raw and normalized dissolved data. Results reflect outcome when CS_2 is imposed on bottles by sulfur-cured septa.

		FeS			FeS2			Cinders			Blank
		9-1	9-2	9-3	9-4	9-5	9-6	9-7	9-8	9-9	9-10
Raw (µmol/L)	H2S	**>6.30**	**>6.77**	**>6.49**	**>6.45**	**>6.23**	**>5.89**	**>27.70**	**>53.67**	**>11.69**	0.00
	COS	0.00	0.00	0.00	0.00	0.00	0.00	*coelute*	*coelute*	*coelute*	0.12
	CH3SH	4.91	7.24	4.47	5.97	8.03	6.37	*3.40*	coelute	0.84	0.00
	Eth-SH	0.03	0.02	0.02	0.00	0.00	0.00	*2.46*	*6.27*	0.28	0.00
	DMS	0.26	0.52	0.13	0.00	0.00	0.00	0.00	0.00	0.00	0.00
	CS2	0.01	0.03	0.07	0.11	0.29	0.11	4.14	1.59	3.53	3.21
	DMDS	0.32	0.32	0.19	0.32	0.87	0.71	2.26	0.00	0.00	0.00
Normalized (µmol/L)	H2S	**>3.70**	**>4.30**	**>3.36**	**>6.60**	**>4.13**	**>5.80**	**>19.29**	**>32.97**	**>4.87**	NA
	COS	0.00	0.00	0.00	0.00	0.00	0.00	*coelute*	*coelute*	*coelute*	NA
	CH3SH	2.89	4.59	2.31	6.10	5.33	6.28	*2.37*	*coelute*	0.35	NA
	Eth-SH	0.02	0.01	0.01	0.00	0.00	0.00	*1.72*	*3.85*	0.11	NA
	DMS	0.15	0.33	0.07	0.00	0.00	0.00	0.00	0.00	0.00	NA
	CS2	0.01	0.02	0.04	0.11	0.19	0.11	2.88	0.98	1.47	NA
	DMDS	0.19	0.20	0.10	0.33	0.58	0.70	1.57	0.00	0.00	NA

Table 9: Results from Experiment 9. Both raw and normalized dissolved data. Italics represent values estimated from coeluted peaks. Results reflect outcome when CS_2 is imposed on bottles by sulfur-cured septa.

		FeS			FeS2			Cinders			Blank
		10-1	10-2	10-3	10-4	10-5	10-6	10-7	10-8	10-9	10-10
Raw (µmol/L)	H2S	30.32	**>48.77**	**>49.97**	16.19	14.55	13.22	**>72.53**	**>78.58**	**>101.25**	0.00
	COS	*coelute*	*coelute*	*coelute*	1.21	0.89	0.62	*coelute*	*coelute*	*coelute*	0.03
	CH3SH	2.40	2.97	3.68	5.13	4.87	3.46	0.34	0.75	2.01	0.00
	Eth-SH	0.01	0.01	0.02	0.03	0.03	0.04	0.00	0.00	0.64	0.00
	DMS	0.00	0.00	0.00	0.00	0.00	0.00	0.00	0.00	0.00	0.00
	CS2	0.00	0.00	0.00	0.02	0.03	0.06	3.80	3.29	3.95	2.00
	DMDS	0.00	0.00	0.00	0.02	0.35	0.53	0.18	0.00	0.00	0.00
Normalized (µmol/L)	H2S	19.47	**>31.94**	**>23.35**	9.63	6.04	8.15	**>37.39**	**>28.36**	**>27.38**	NA
	COS	*coelute*	*coelute*	*coelute*	0.72	0.37	0.38	*coelute*	*coelute*	*coelute*	NA
	CH3SH	1.54	1.94	1.72	3.05	2.02	2.13	0.18	0.27	0.54	NA
	Eth-SH	0.01	0.01	0.01	0.02	0.01	0.03	0.00	0.00	0.17	NA
	DMS	0.00	0.00	0.00	0.00	0.00	0.00	0.00	0.00	0.00	NA
	CS2	0.00	0.00	0.00	0.01	0.01	0.04	1.96	1.19	1.07	NA
	DMDS	0.00	0.00	0.00	0.01	0.15	0.32	0.09	0.00	0.00	NA

Table 10: Results from Experiment 10. Both raw and normalized dissolved data. Results reflect outcome when CS_2 is imposed on bottles by sulfur-cured septa.

	Experiment 12: Nitrogen								
	Dry			D.I. water			Synthetic CP water		
	12-1	12-2	12-3	12-4	12-5	12-6	12-7	12-8	12-9
SO_2	Y	Y	Y	N	N	N	N	N	N
CS_2	Y	Y	Y	Y	Y	Y	Y	Y	Y
	Experiment 13: CO_2 and H_2 Mix								
	Dry			D.I. water			Synthetic CP water		
	13-1	13-2	13-3	13-4	13-5	13-6	13-7	13-8	13-9
SO_2	Y	Y	Y	N	N	N	N	N	N
CS_2	Y	Y	Y	Y	Y	Y	Y	Y	Y

Table 11: Off gassing of butyl stoppers in various blank conditions.

New vs. Old Stoppers			
		SO_2	CS_2
New	14-1	Y	Y
	14-2	Y	Y
	14-3	Y	Y
Old	14-4	N	N
	14-5	Y	very tiny
	14-6	N	N

Table 12: Experiment 14 results: Bottles capped with either old or new stoppers and subjected to one cycle through the autoclave.

		FeS			FeS2			Cinders			Blank
		15-1	15-2	15-3	15-4	15-5	15-6	15-7	15-8	15-9	15-10
Raw (µmol/L)	H2S	0.81	3.35	11.13	0.00	0.38	2.30	**>102.61**	**>76.56**	**>137.34**	0.00
	COS	0.00	0.00	0.00	0.00	0.00	0.00	0.00	0.00	0.00	0.00
	CH3SH	0.00	0.00	0.00	0.00	0.00	0.00	2.52	1.26	12.58	0.00
	Eth-SH	0.00	0.00	0.00	0.00	0.00	0.00	1.35	0.42	4.18	0.00
	DMS	0.00	0.00	0.00	0.00	0.00	0.00	0.00	0.00	0.00	0.00
	CS2	0.00	0.00	0.00	0.00	0.00	0.00	0.35	0.21	0.57	0.00
	DMDS	0.00	0.00	0.00	0.00	0.00	0.00	0.00	0.00	0.00	0.00
Normalized (µmol/L)	H2S	0.41	1.77	8.37	0.00	0.22	1.24	**>41.37**	**>47.85**	**>63.29**	NA
	COS	0.00	0.00	0.00	0.00	0.00	0.00	0.00	0.00	0.00	NA
	CH3SH	0.00	0.00	0.00	0.00	0.00	0.00	1.01	0.79	5.80	NA
	Eth-SH	0.00	0.00	0.00	0.00	0.00	0.00	0.54	0.27	1.93	NA
	DMS	0.00	0.00	0.00	0.00	0.00	0.00	0.00	0.00	0.00	NA
	CS2	0.00	0.00	0.00	0.00	0.00	0.00	0.14	0.13	0.26	NA
	DMDS	0.00	0.00	0.00	0.00	0.00	0.00	0.00	0.00	0.00	NA

Table 13: Results from Experiment 15. Both raw and normalized dissolved data. No additional sulfur was imposed on the system (i.e. CS_2 did not degas from the septa).

Figures

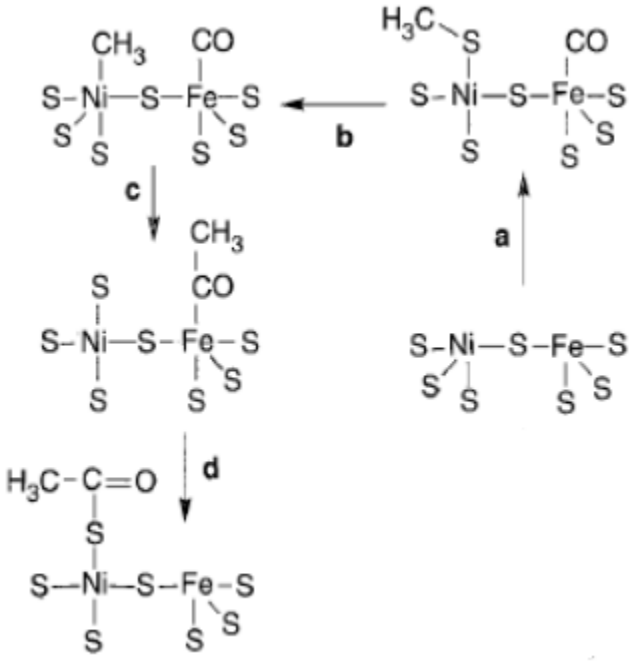

Figure 1: Representation adapted from Huber and Wächtershäuser (1997) of a primitive reductive acetyl-CoA pathway. The acetyl group can leave the reaction center, forming thioacetic acid.

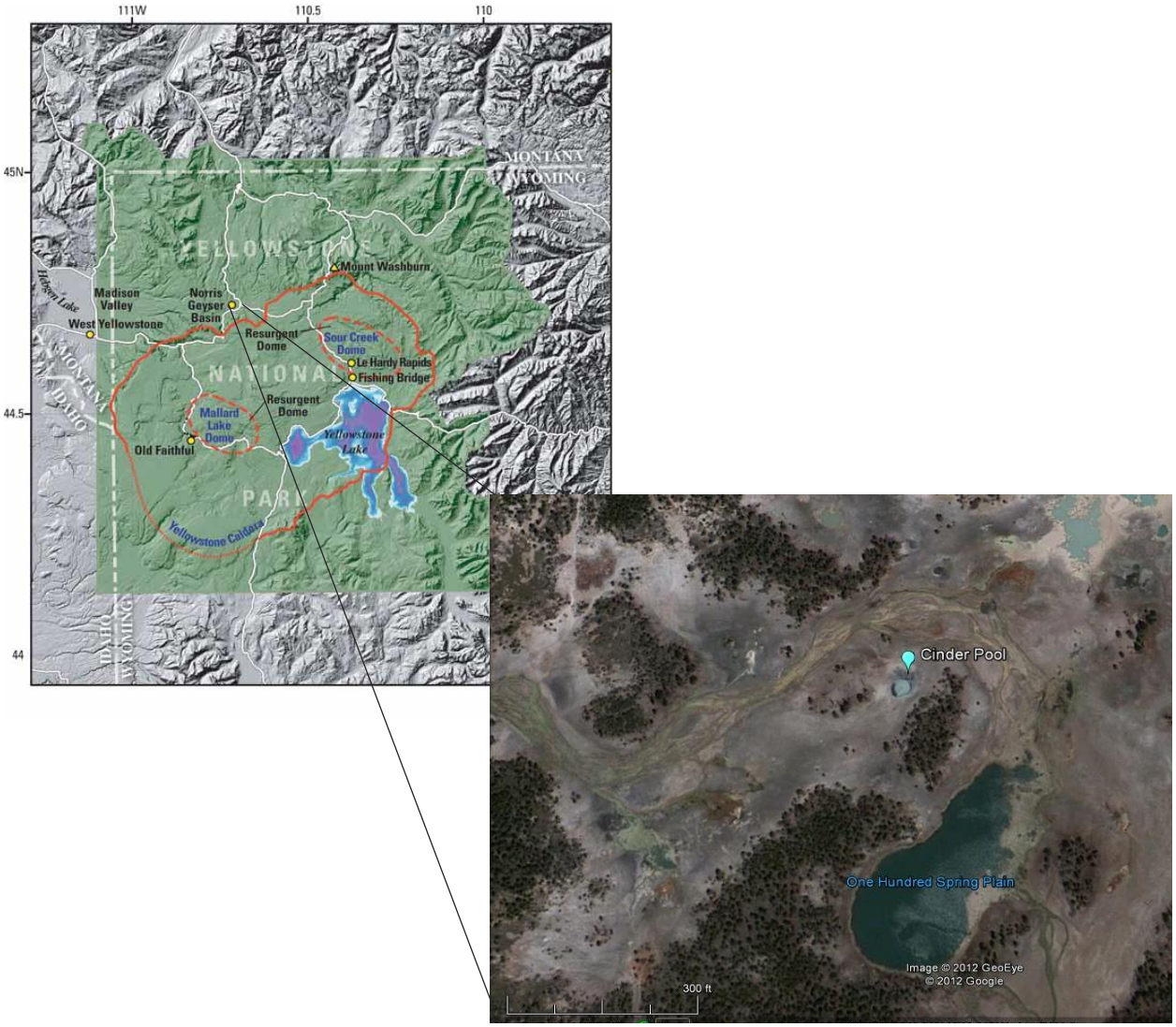

Figure 2: Map of Norris Gesyer Basin within Yellowstone National Park. Detail Cinder Pool in the One Hundred Spring Plain. Map is a reproduction from USGS Fact Sheet 100-03, 2004, and satellite imagery is courtesy of Google Earth.

Figure 3: Cinder Pool in September of 2010

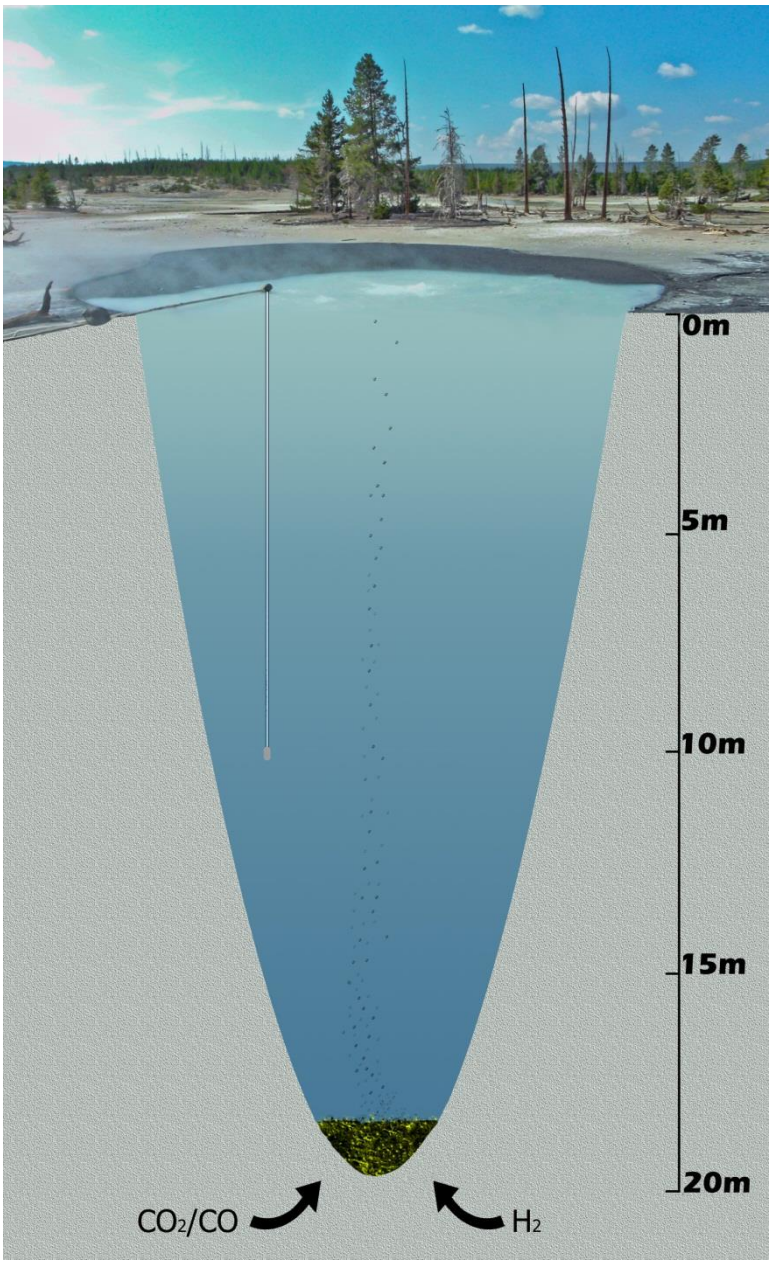

Figure 4: This is a graphic interpretation of Cinder Pool. Note that in reality the depth beneath the molten sulfur layer at the bottom is not known, and is merely depicted here to show the location of the sulfur/water interface. Water is pumped up the tubing and into the bubble stripping apparatus.

Figure 5: A spherule collected from the surface of Cinder Pool

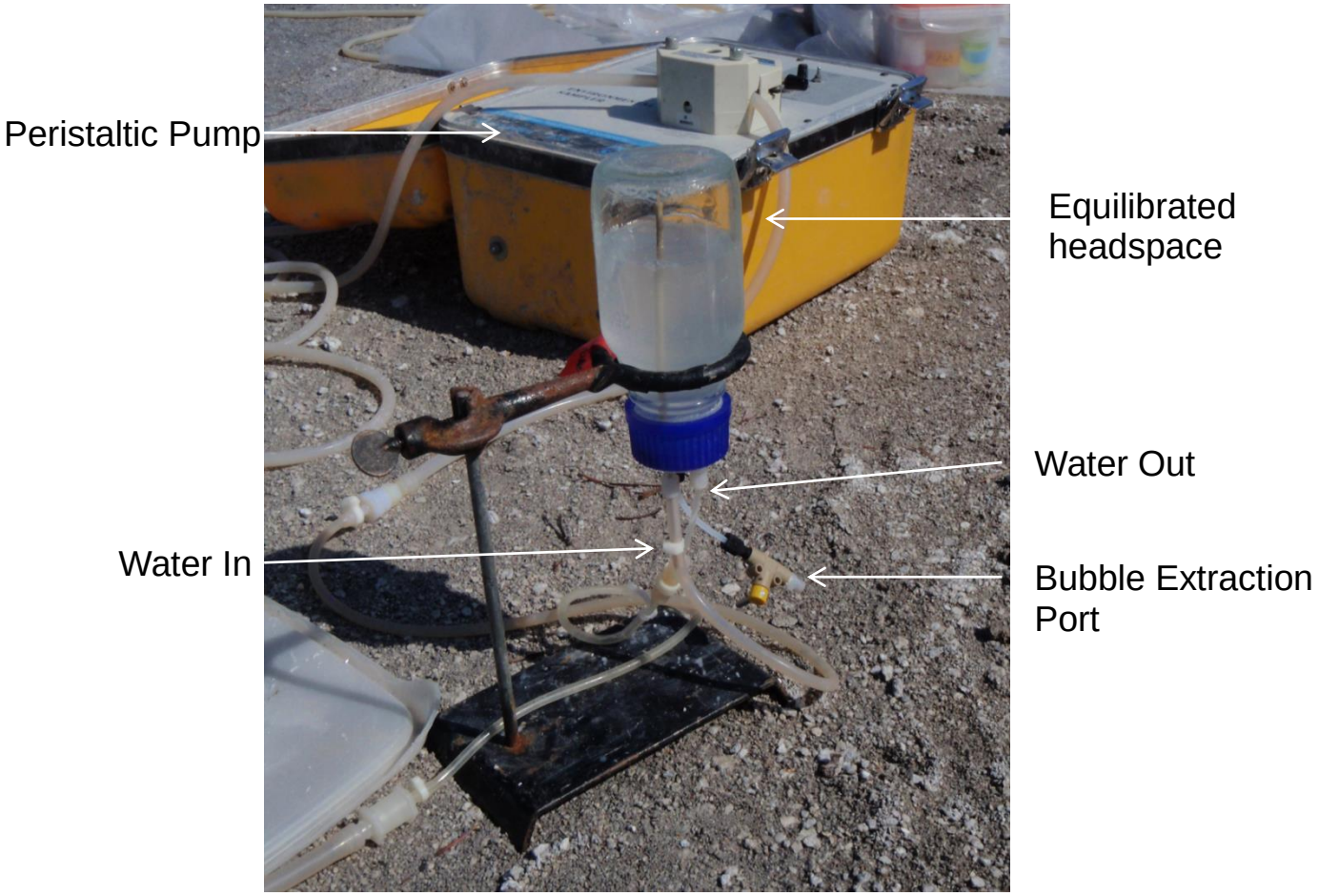

Figure 6: Bubble Stripping Apparatus at Cinder Pool. Water flows continuously into the bottle through the tan tube inside and out through a clear tube at a lower level until the headspace is equilibrated with the dissolved gases. The bubble can then be extracted for immediate analysis or storage in a sealed and sterilized serum bottle.

Figure 7: Subaqueous molten sulfurous material

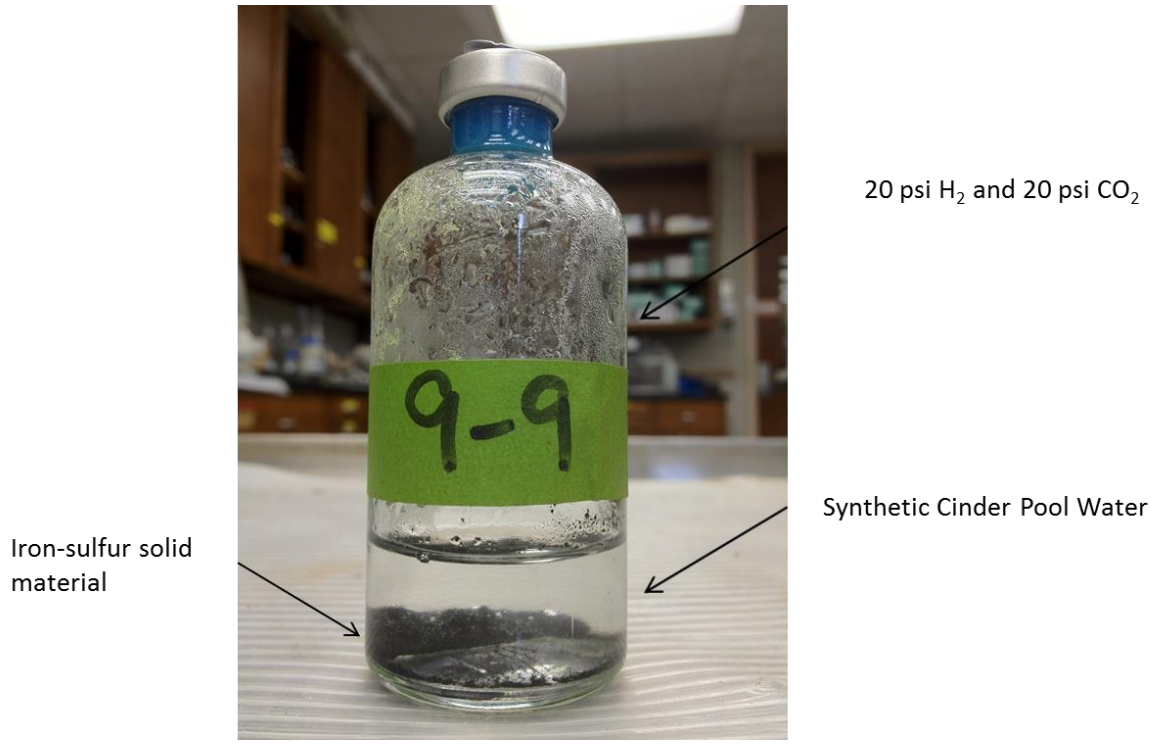

Figure 8: Laboratory microcosm experiment. The solid material in this particular experiment was pulverized cinders from Cinder Pool.

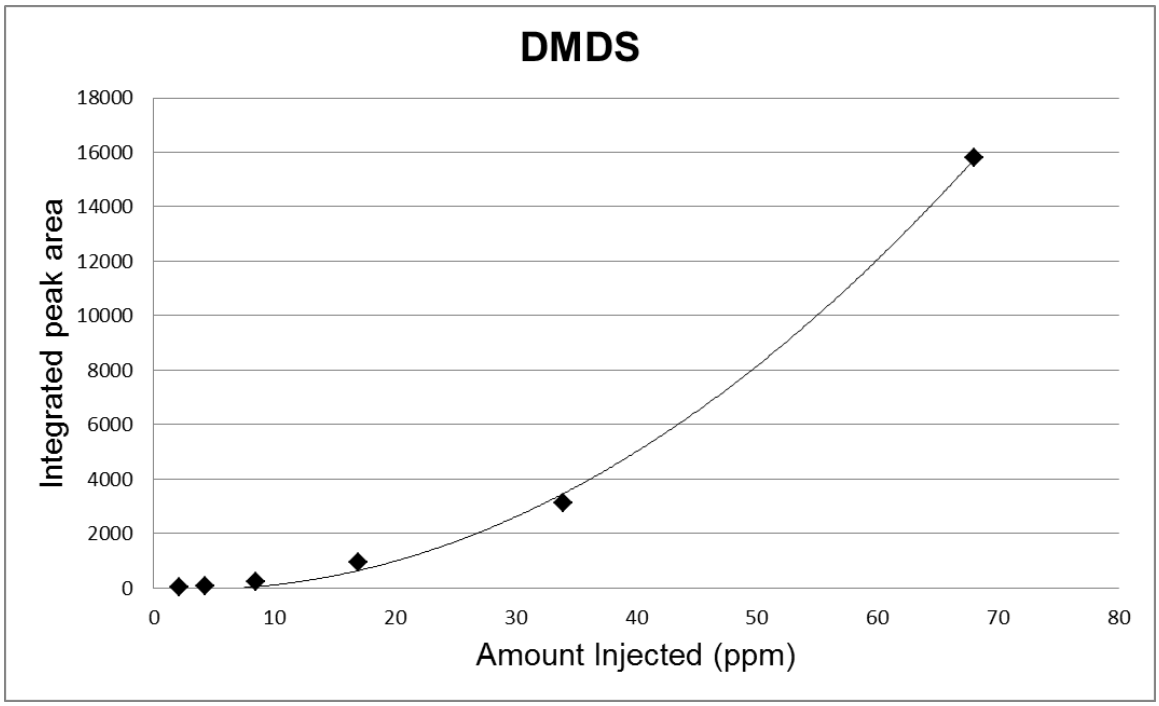

Figure 9: Calibration Curve for dimethyl disulfide, made from dilutions of a 272 ppm DMDS gas standard created in the lab.

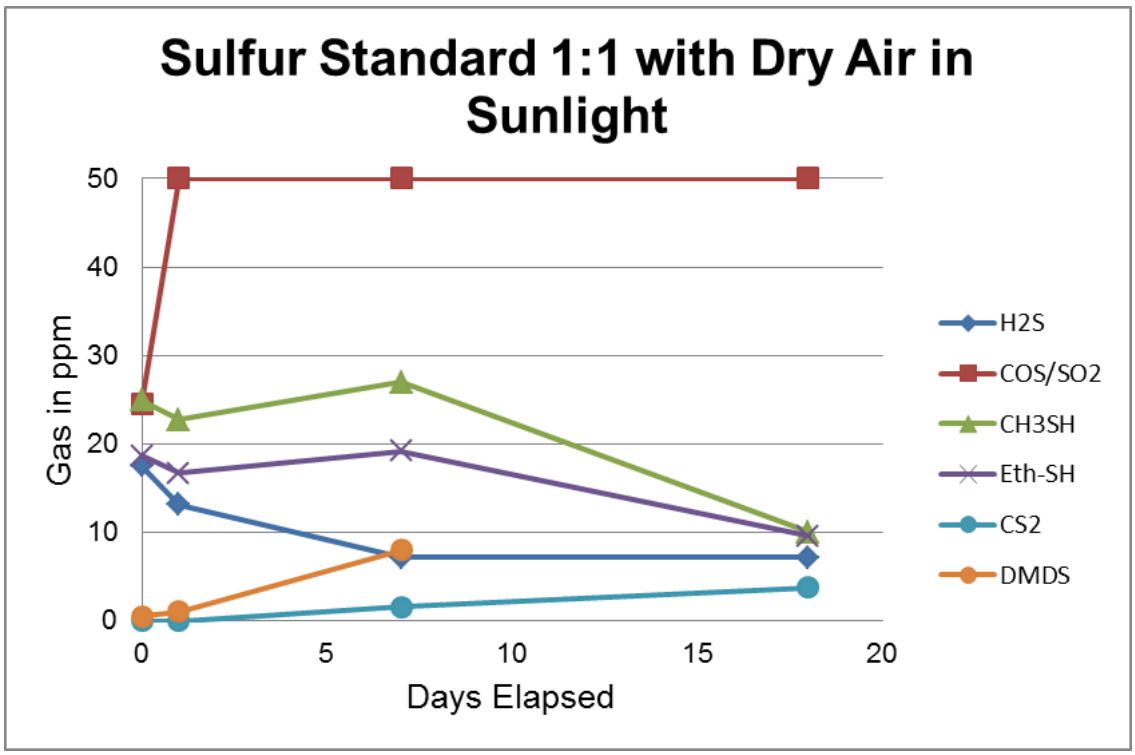

Figure 10: Sulfur gas standard degradation in presence of dry air and sunlight.

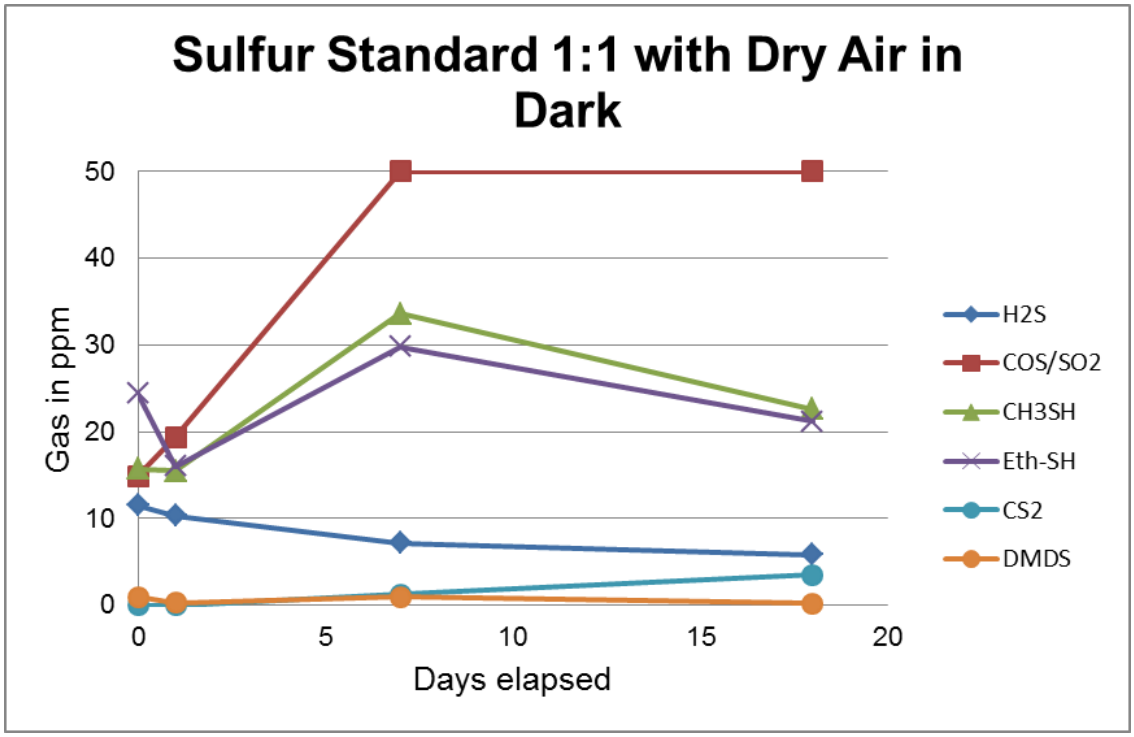

Figure 11: Sulfur gas standard degradation in presence of dry air and total darkness.

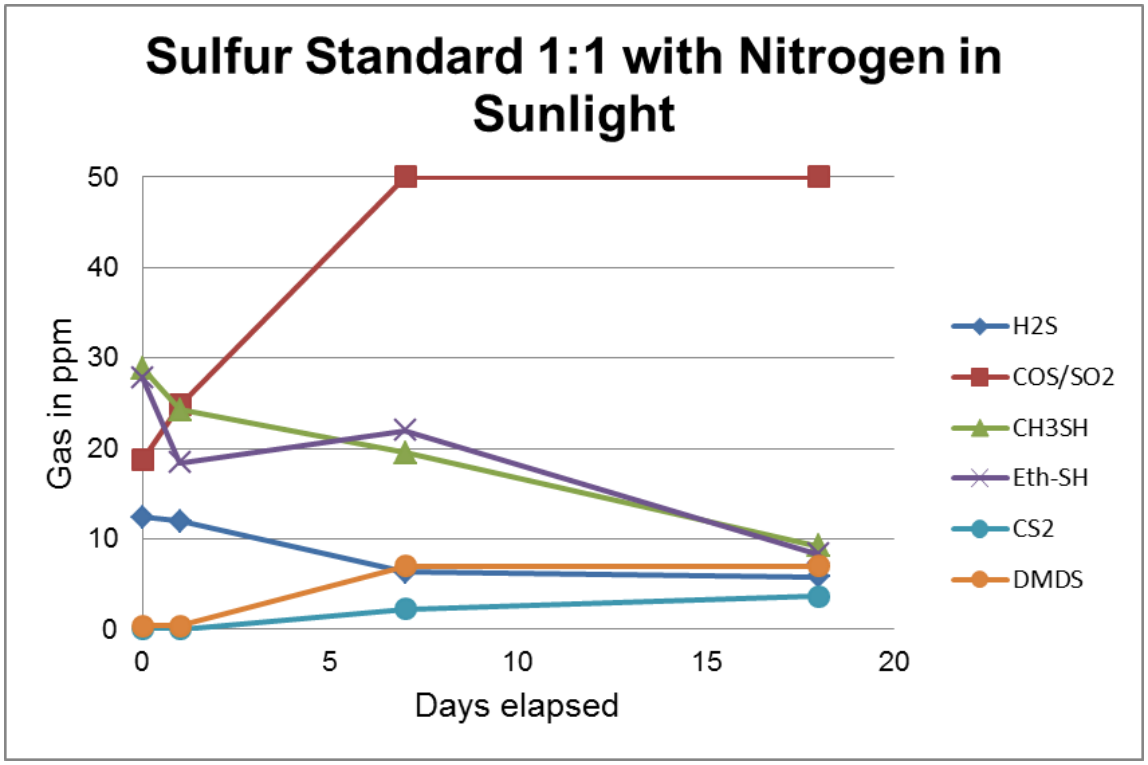

Figure 12: Sulfur gas standard degradation in presence of nitrogen and sunlight.

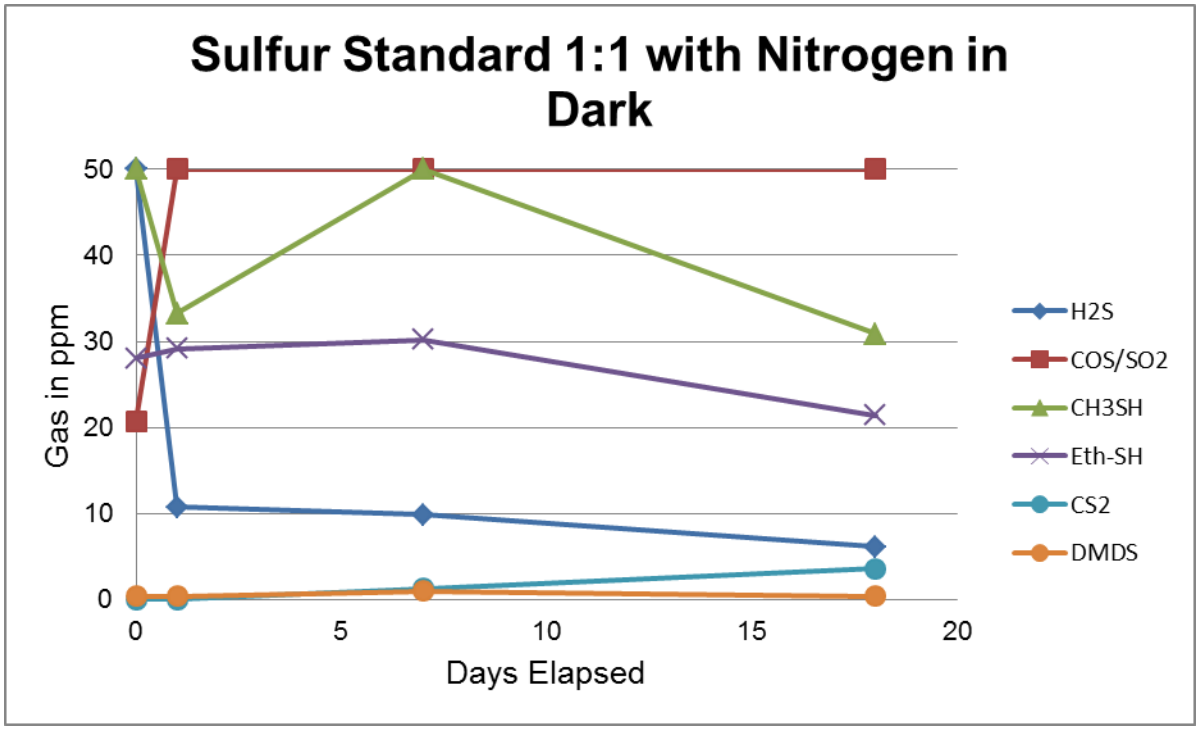

Figure 13: Sulfur gas standard degradation in presence of nitrogen and total darkness.

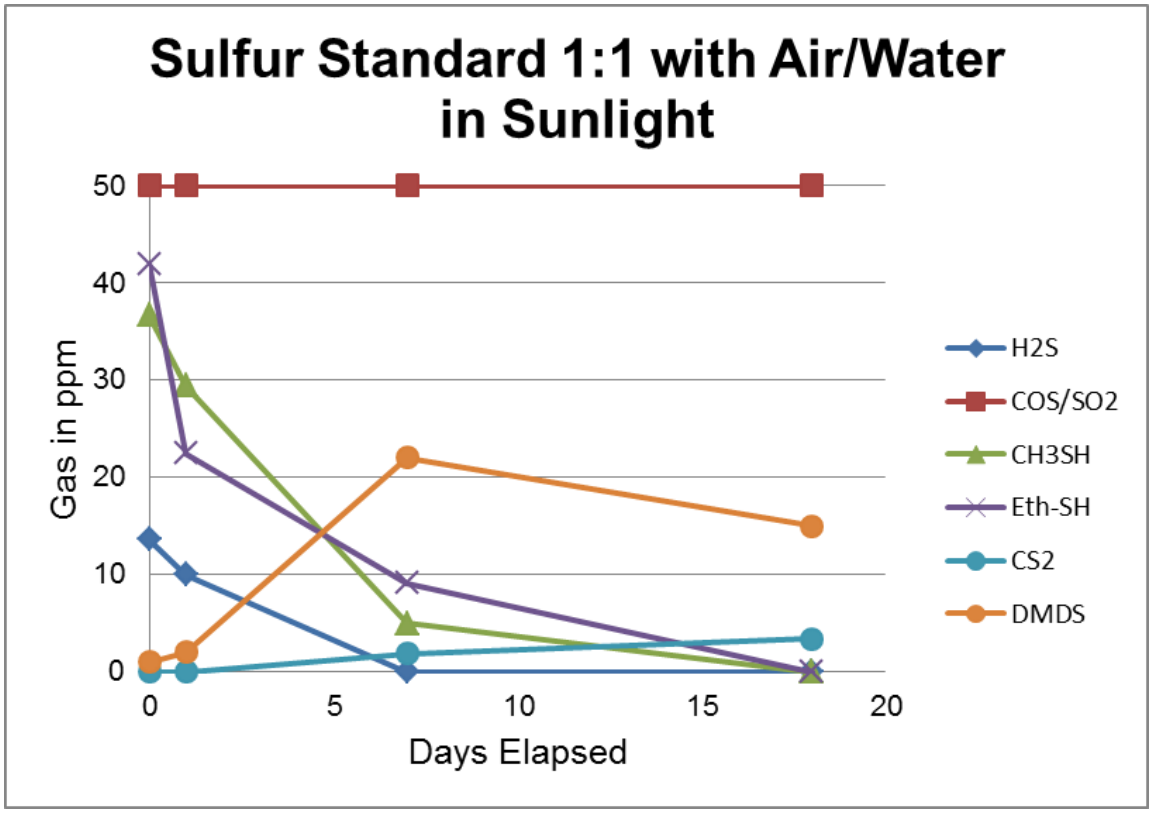

Figure 14: Sulfur gas standard degradation in presence of atmospheric air and water in sunlight.

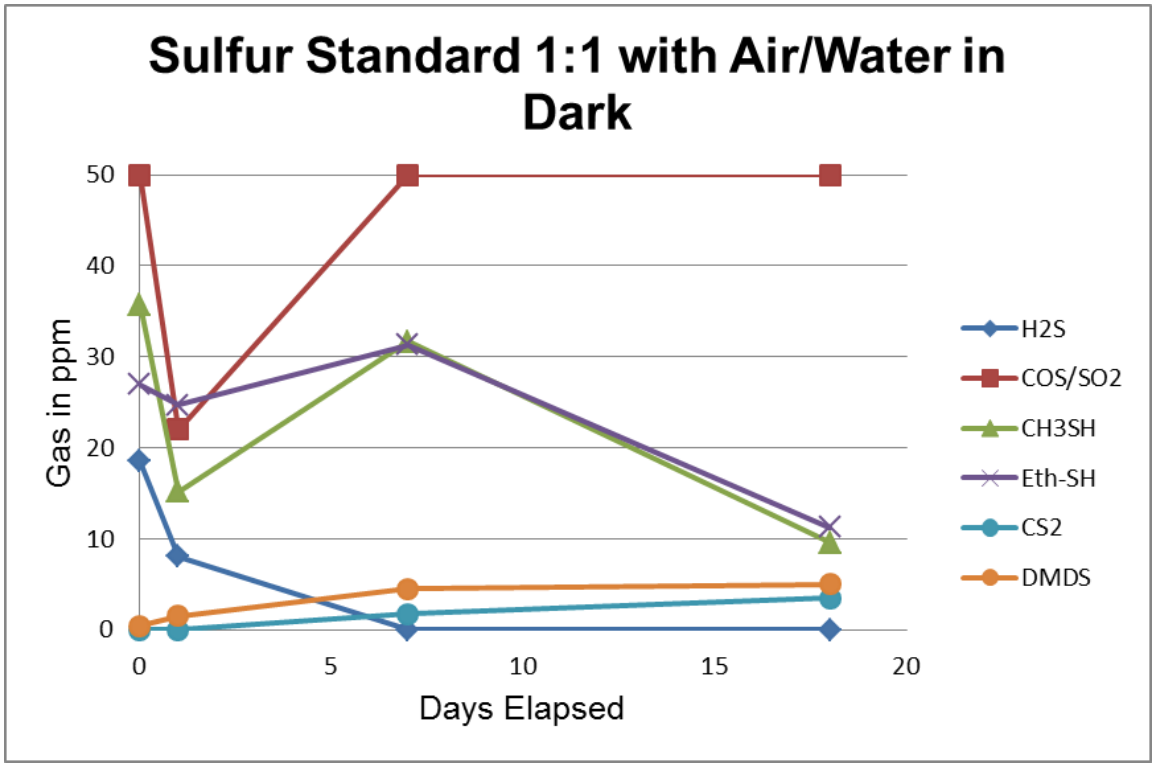

Figure 15: Sulfur gas standard degradation in presence of atmospheric air and water in total darkness.

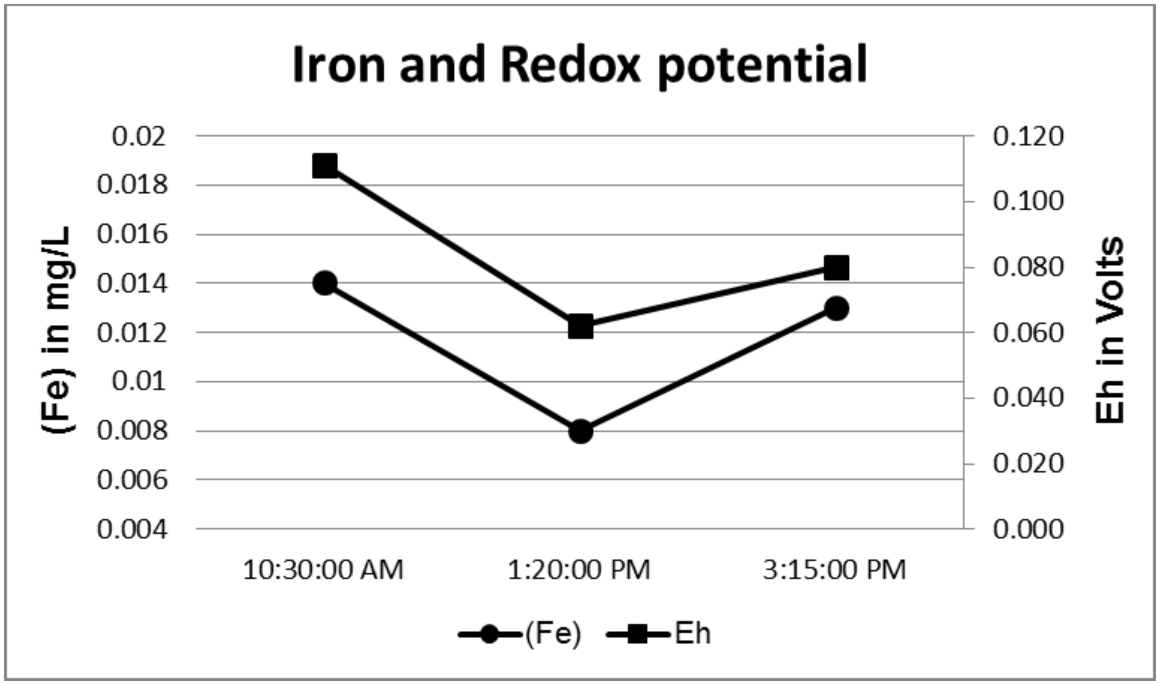

Figure 16: Iron concentrations and redox potential trend over the course of sampling on 09/13/2011.

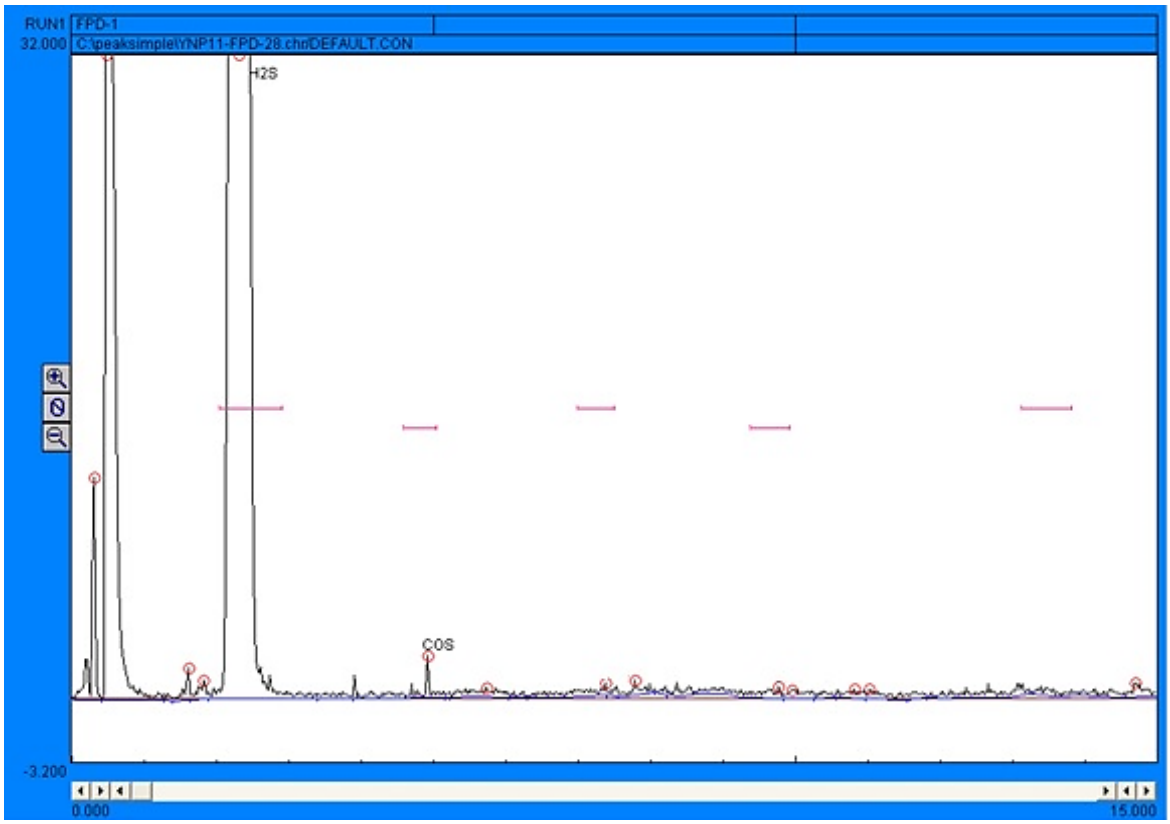

Figure 17: In-situ chromatogram from 3 m deep in Cinder Pool

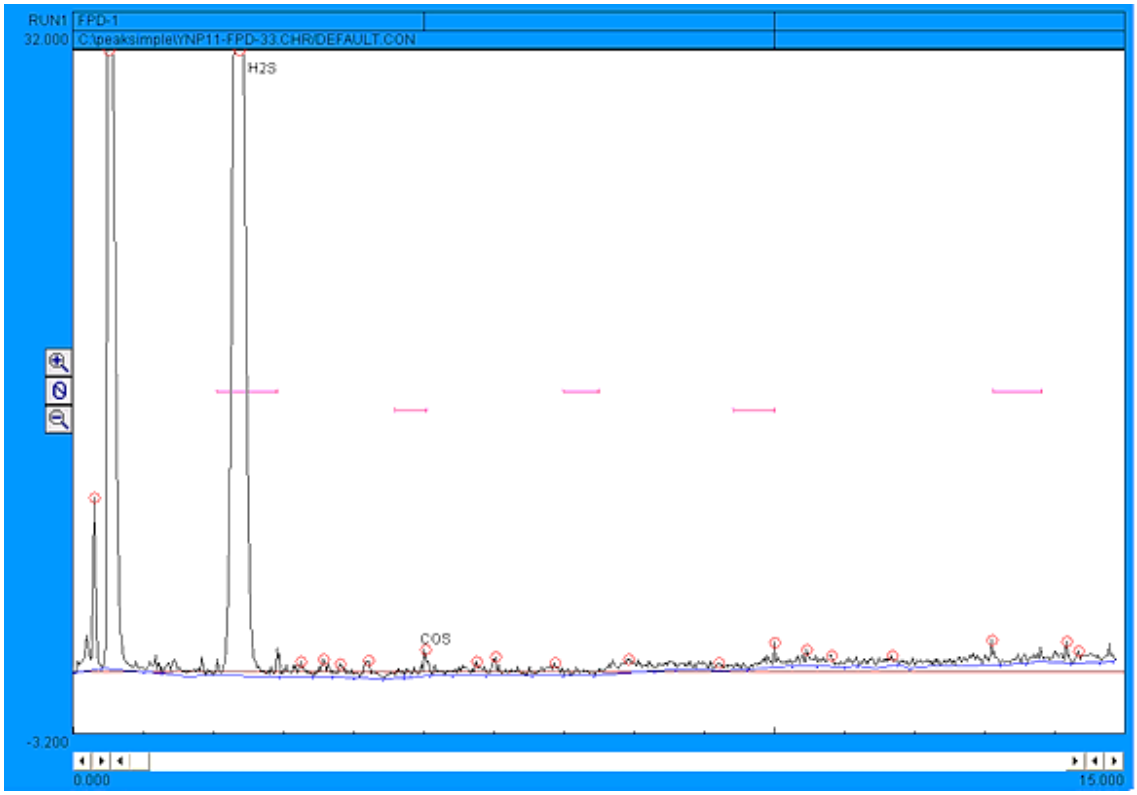

Figure 18: In-situ chromatogram from 17 m deep in Cinder Pool

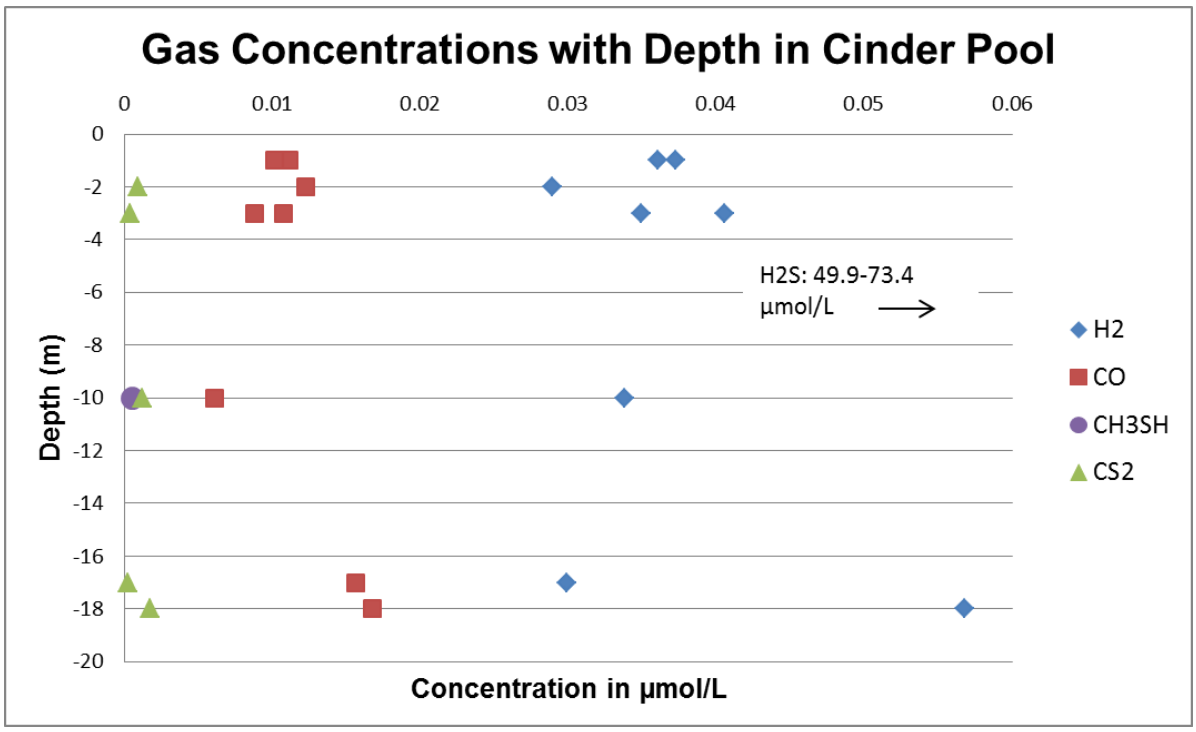

Figure 19: Gas concentrations in Cinder Pool vs. depth. Note that H_2S has not been included due to its concentrations above quantifiable levels for the G.C., and the values obtained for H_2S concentration by titration did not correspond to specific depths.

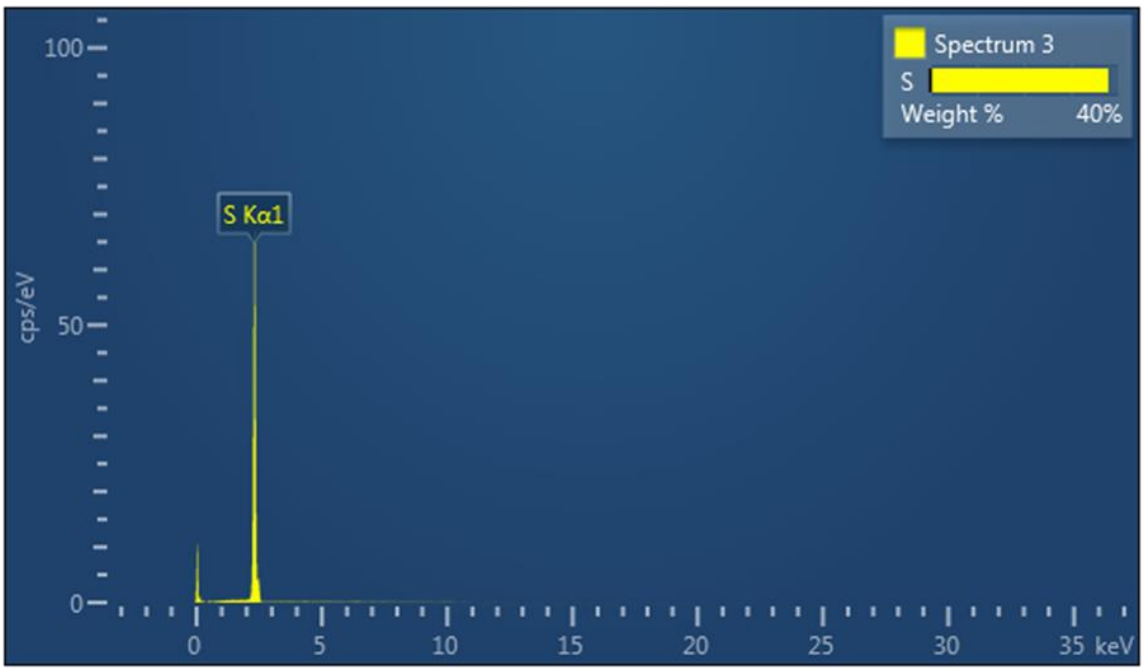

Figure 20: X-ray Spectrum of Cinder Pool bottom material—Site 1.

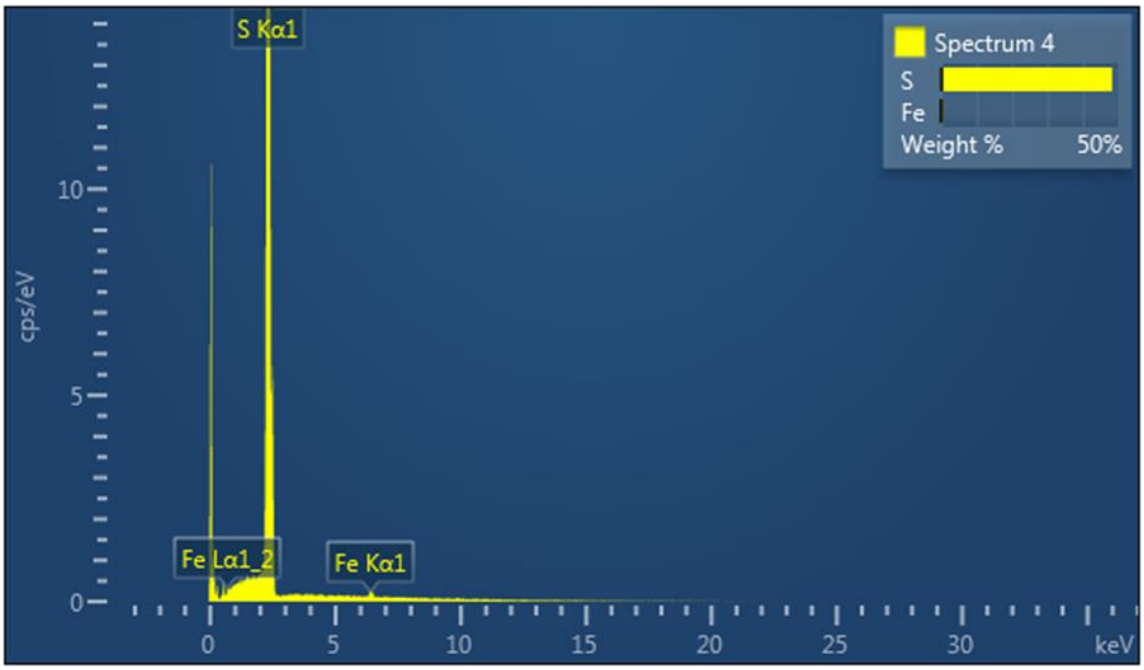

Figure 21: X-ray Spectrum of Cinder Pool bottom material—Site 2.

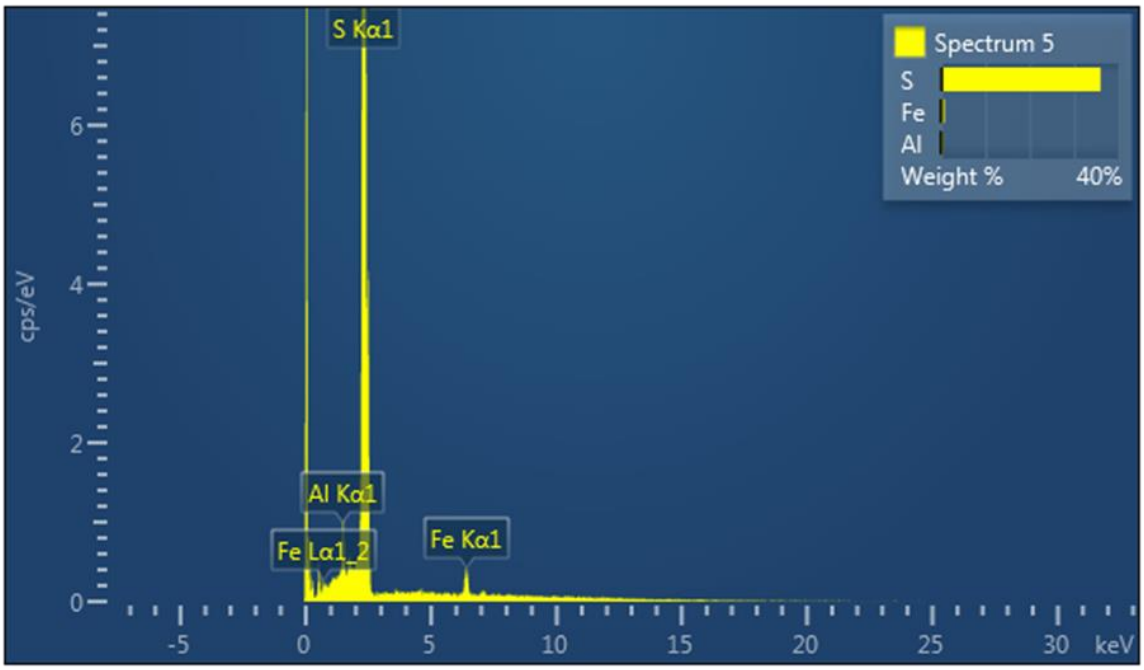

Figure 22: X-ray Spectrum of Cinder Pool bottom material—Site 3.

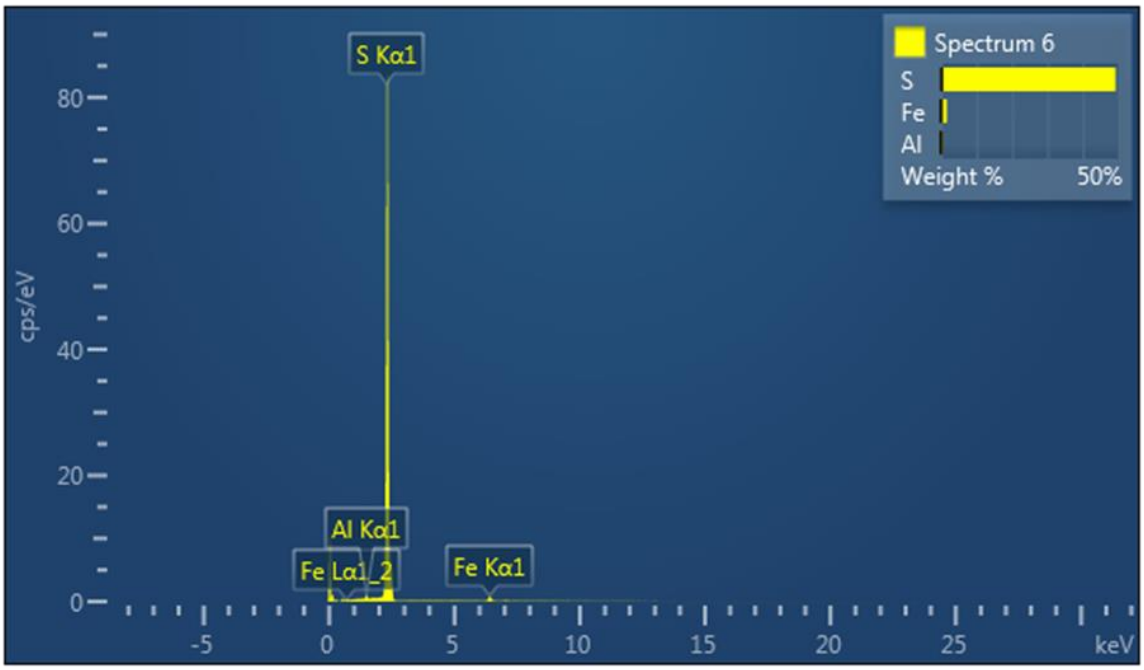

Figure 23: X-ray Spectrum of Cinder Pool bottom material—Site 4.

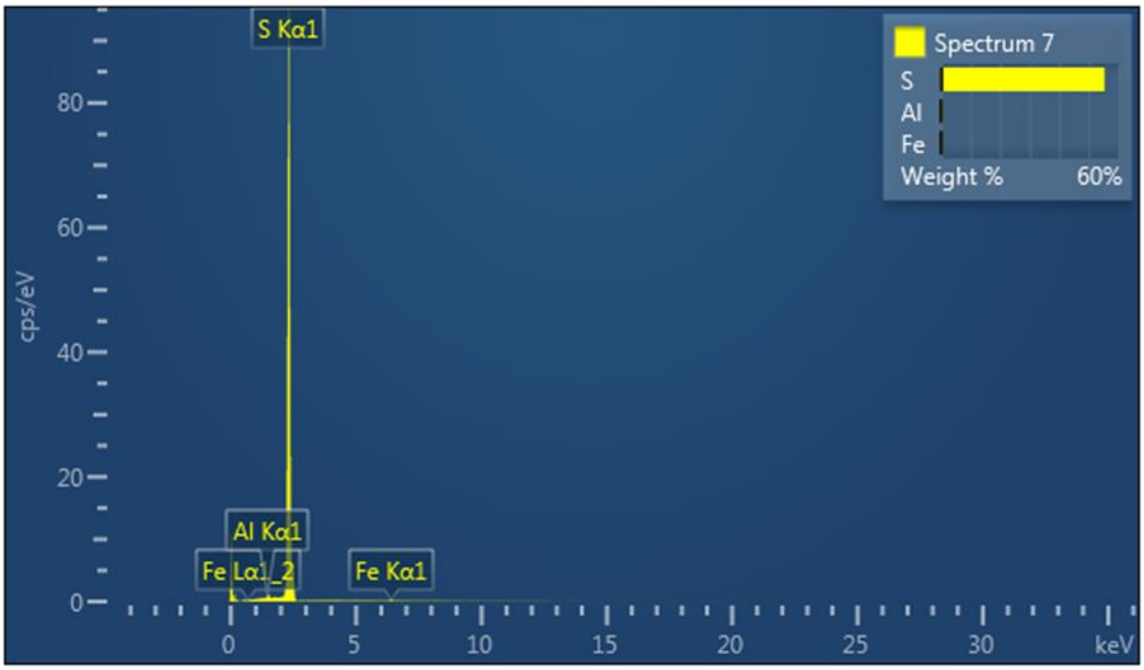

Figure 24: X-ray Spectrum of Cinder Pool bottom material—Site 5.

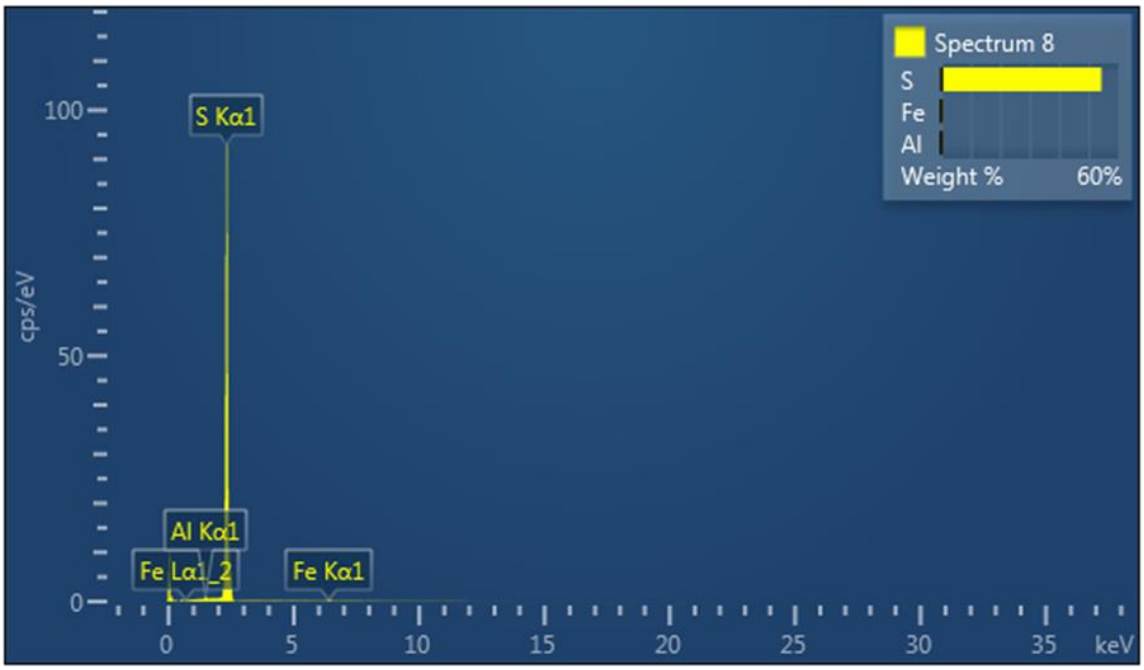

Figure 25: X-ray Spectrum of Cinder Pool bottom material—Site 6.

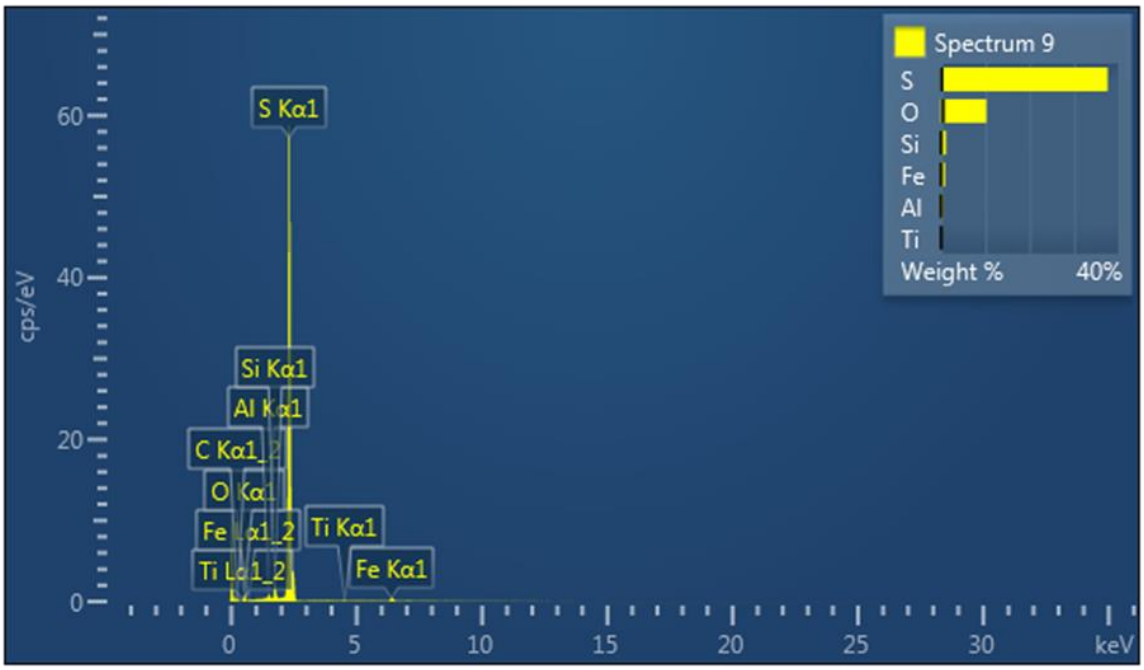

Figure 26: X-ray Spectrum of whole Cinder—Site 7.

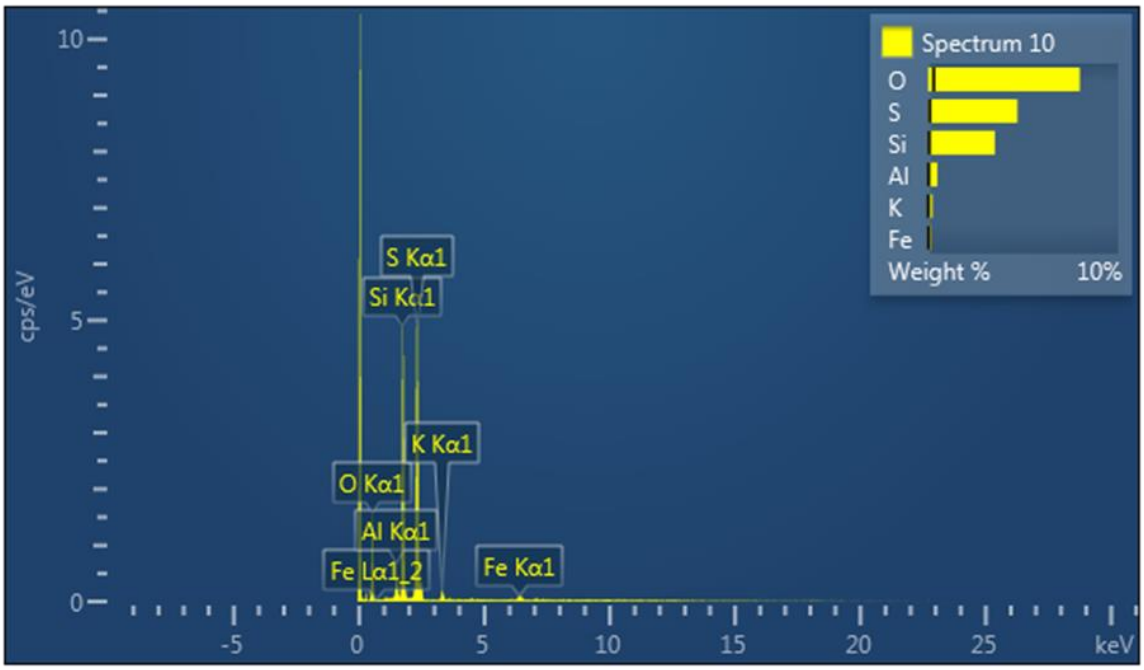

Figure 27: X-ray Spectrum of whole Cinder—Site 8.

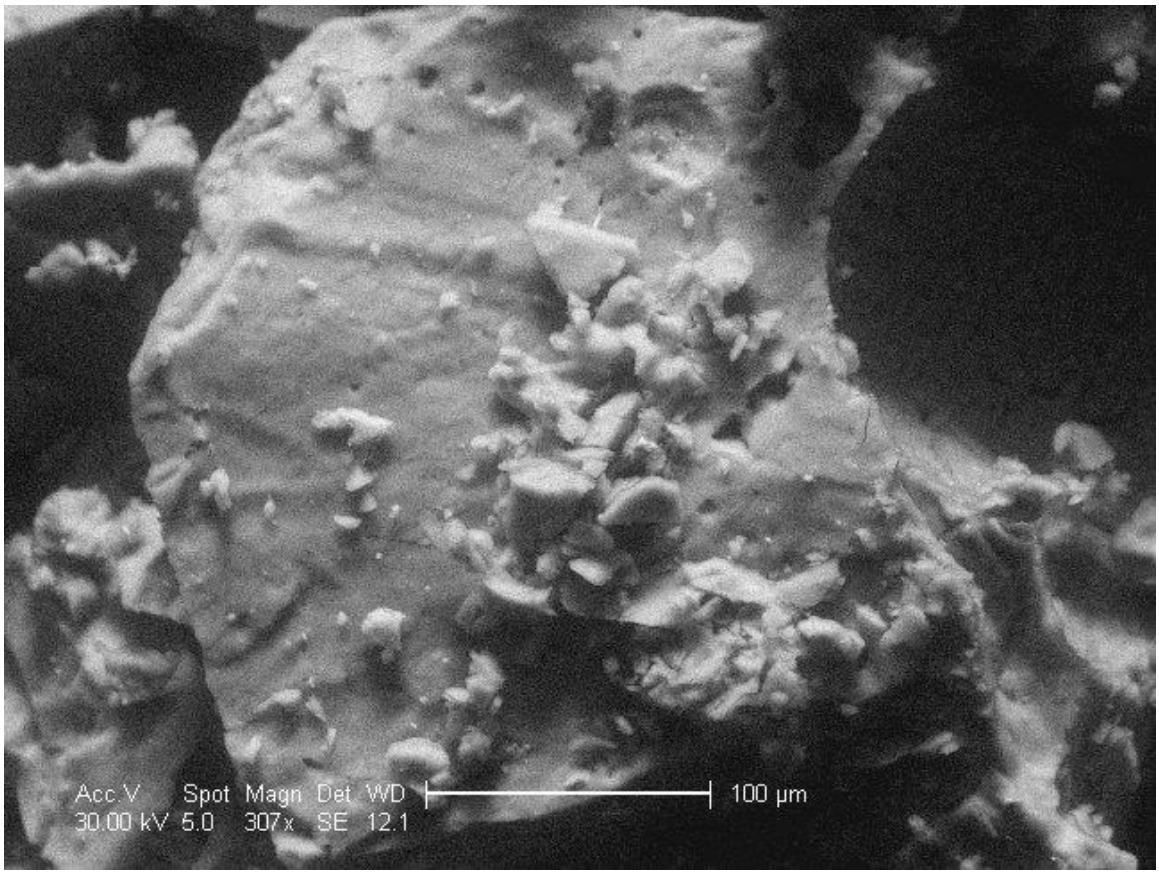

Figure 28: ESEM image of pulverized cinder material from the bottom of the pool

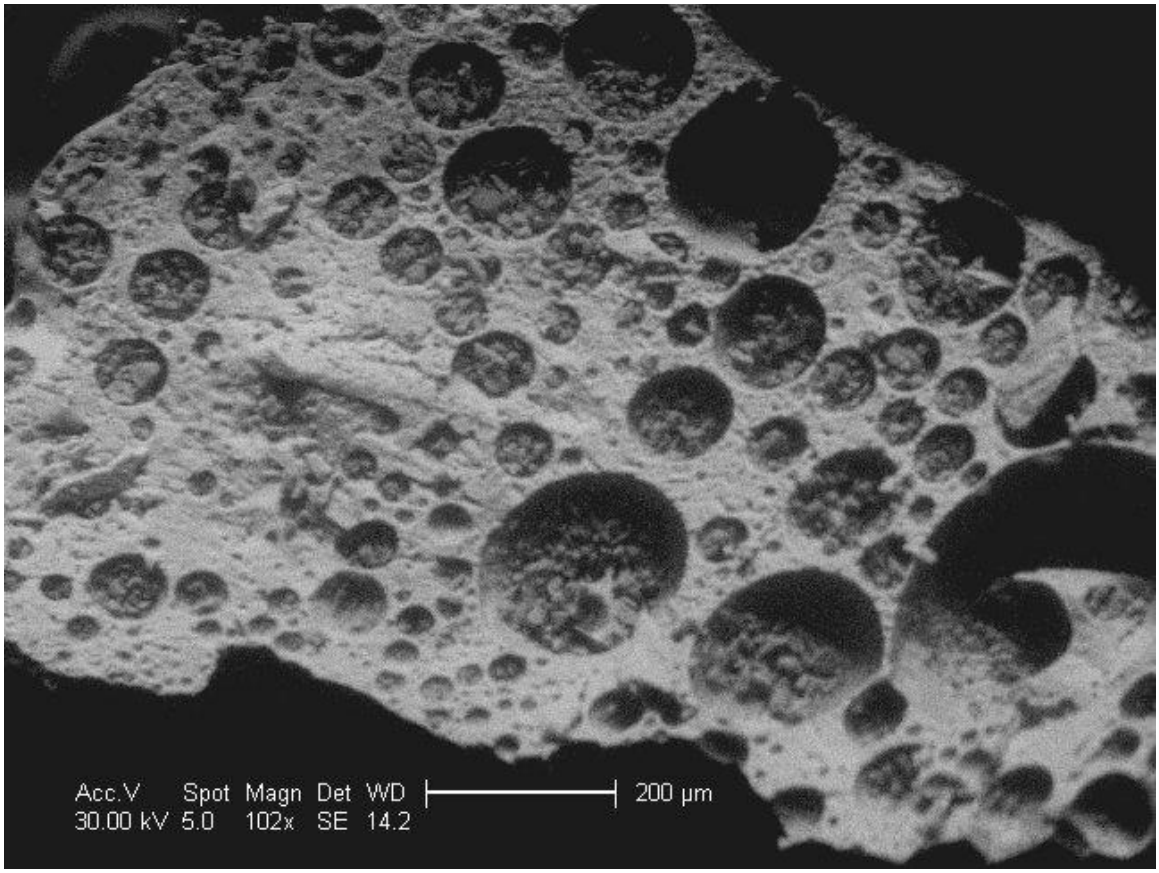

Figure 29: ESEM image of whole Cinder surface.

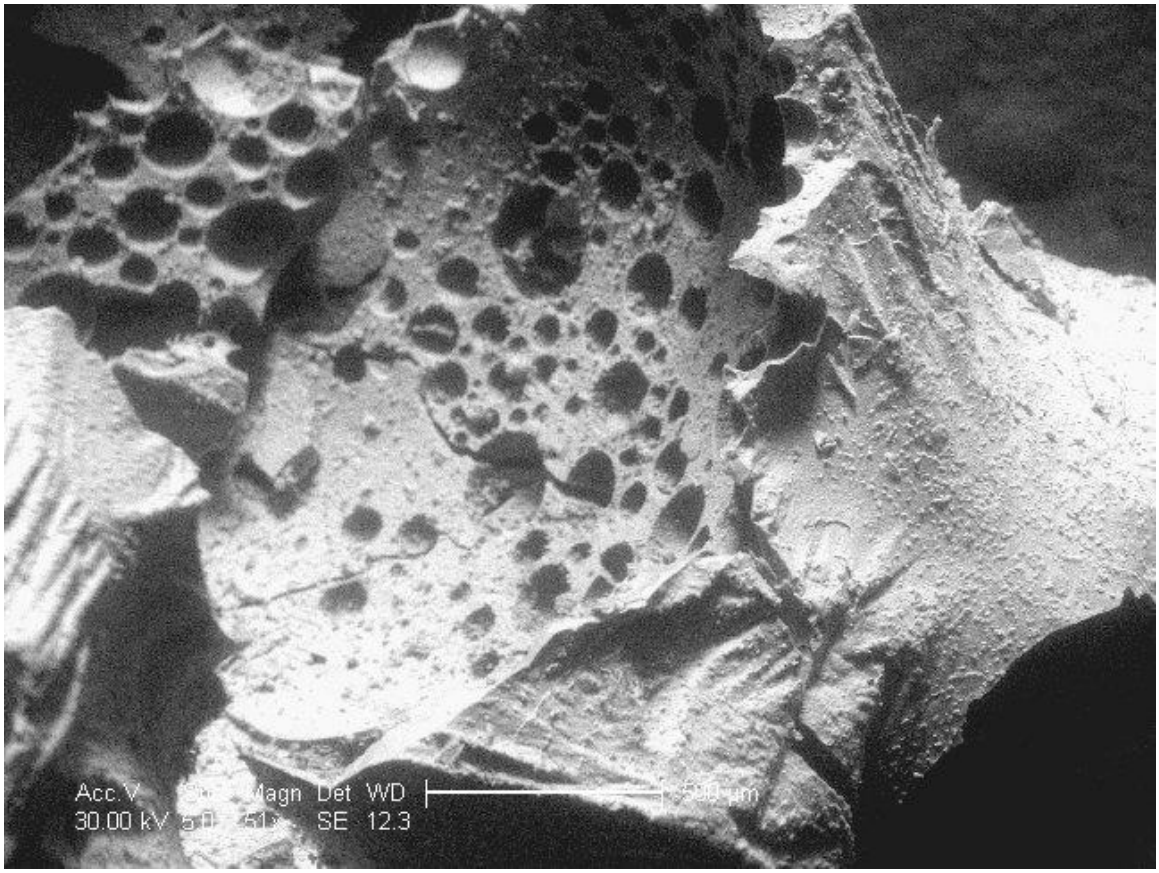

Figure 30: ESEM image of whole Cinder surface.

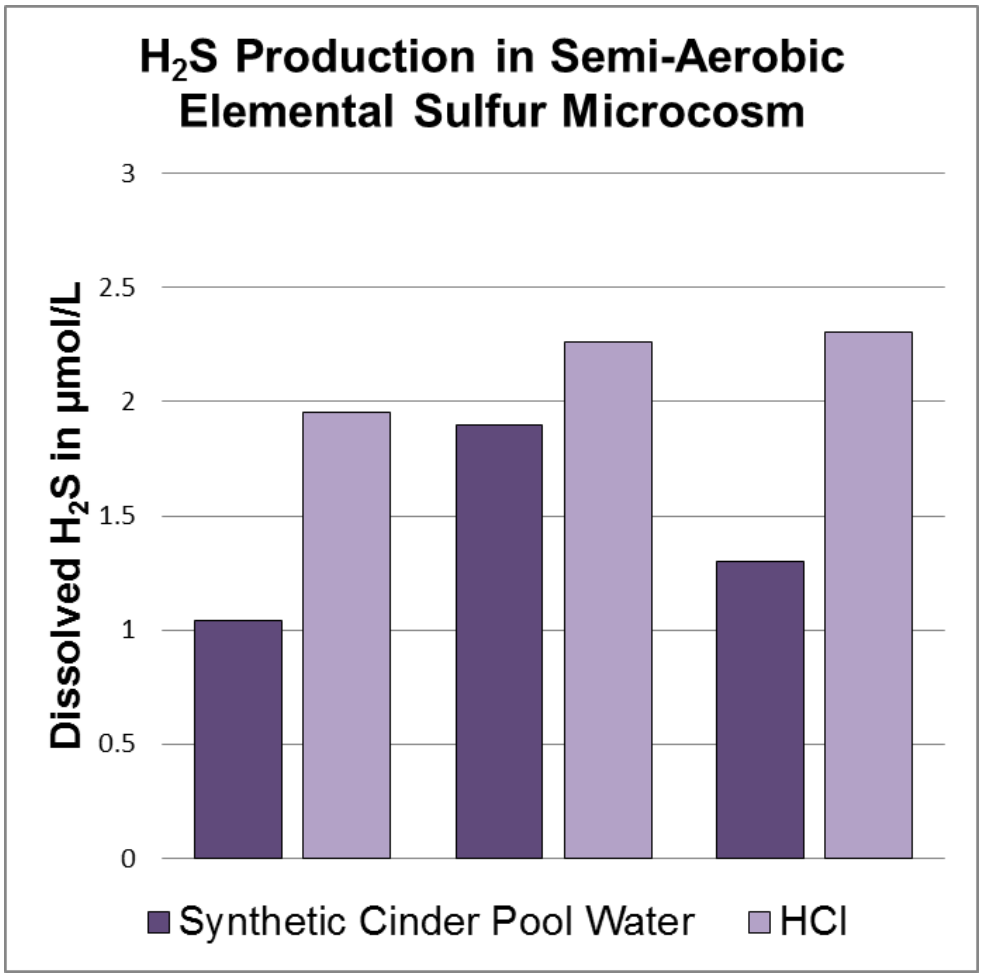

Figure 31: Production of Hydrogen Sulfide gas in semi-aerobic microcosms containing elemental sulfur. Contains 3 replicates each in synthetic Cinder Pool water or dilute HCl. Normalized to 1 g of S^0

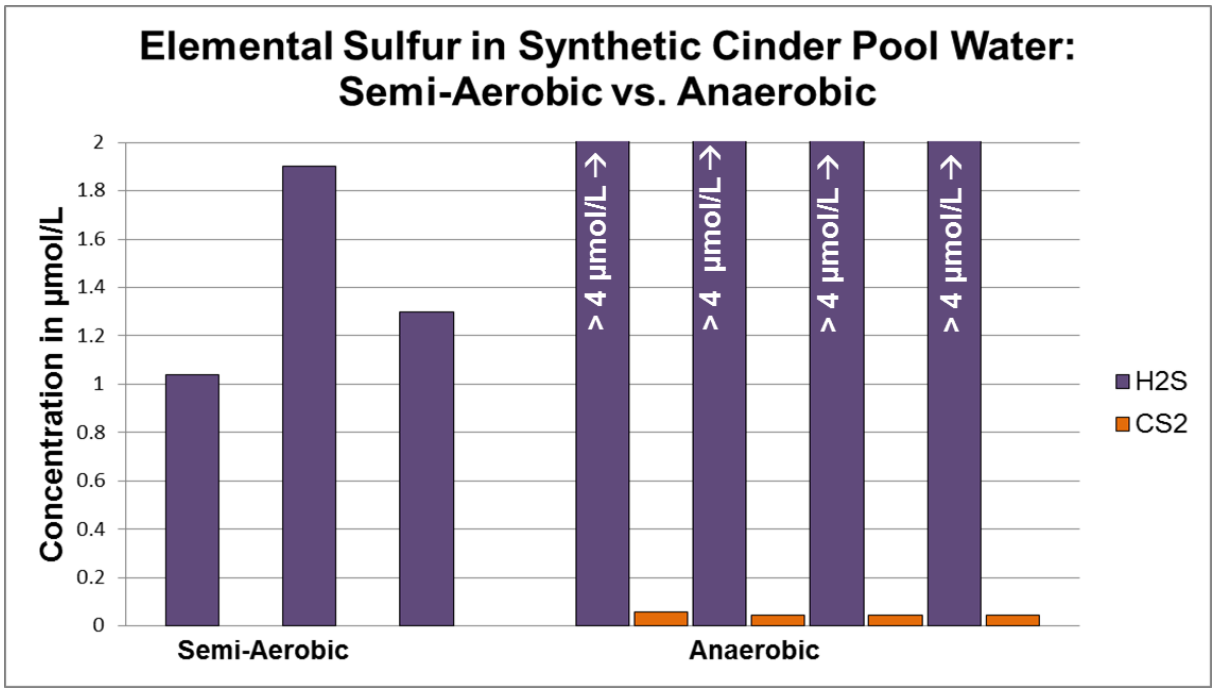

Figure 32: Gases produced in either a semi aerobic or anaerobic environment from synthetic Cinder Pool water and elemental sulfur. Shows 3 semi-aerobic replicates and 4 anaerobic replicates. Normalized to 1 g of S^0.

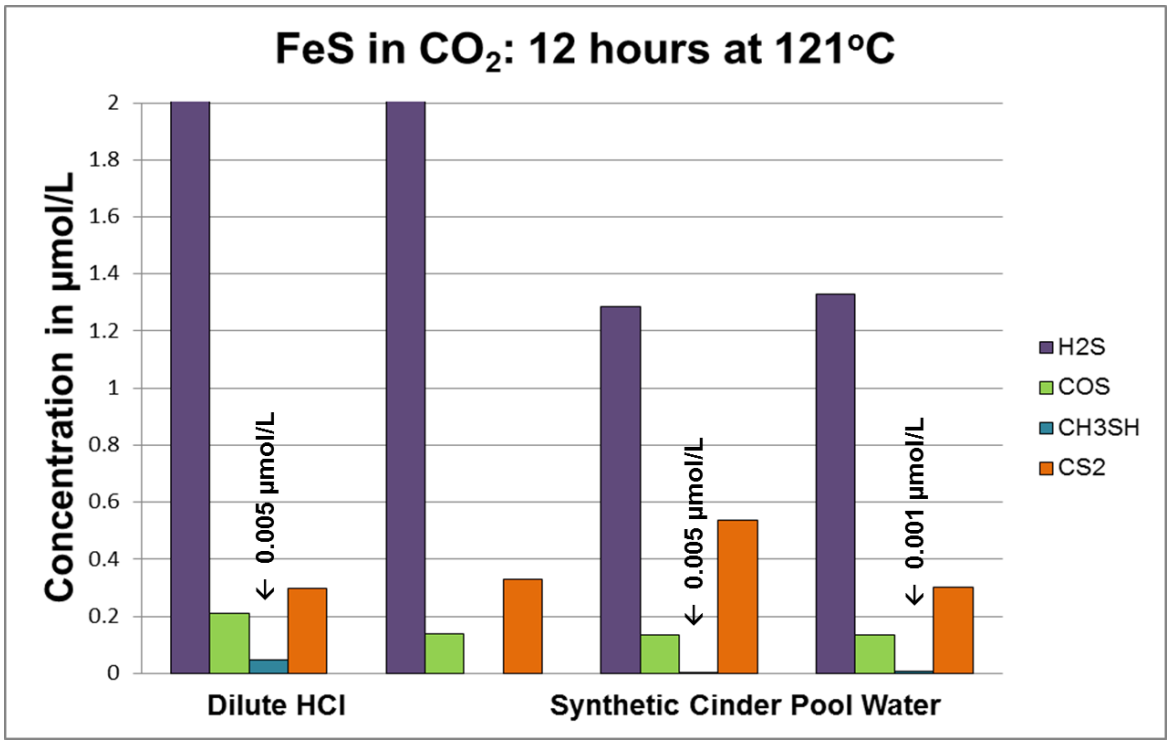

Figure 33: Gases detected in semi-aerobic overnight microcosms using FeS, CO_2, and either dilute HCl or synthetic Cinder Pool water. Normalized to 1 gram of FeS.

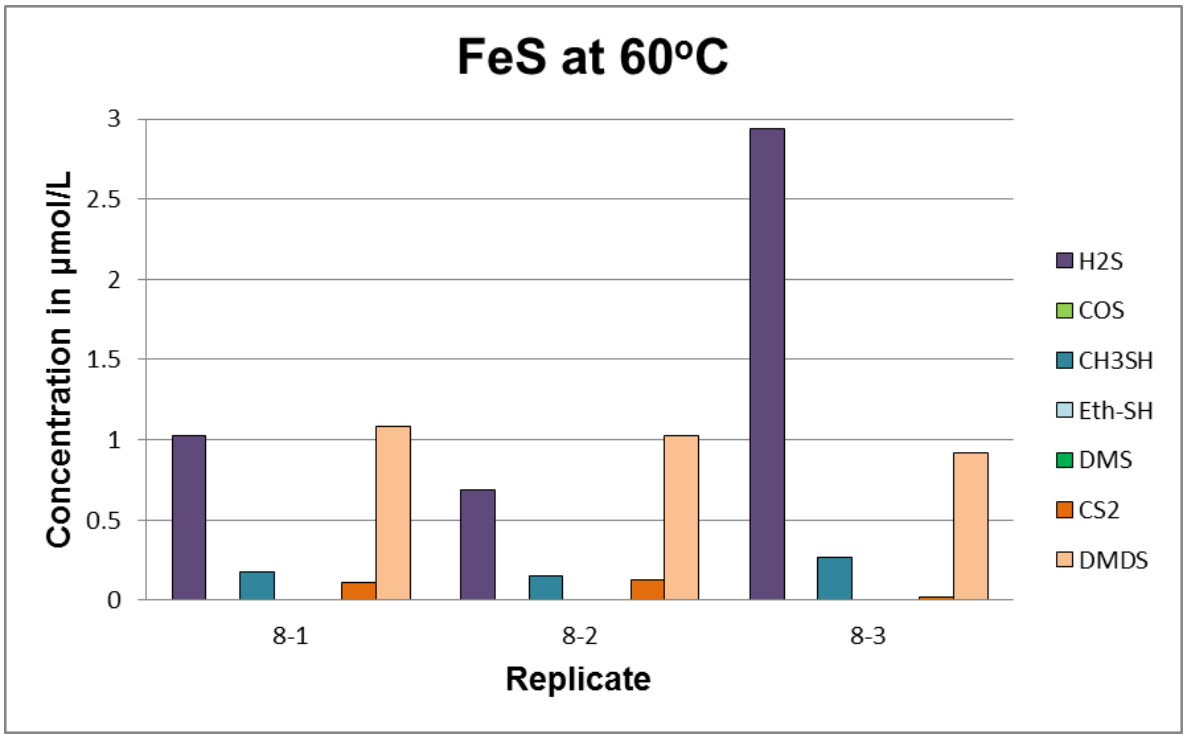

Figure 34: Gases detected in anaerobic microcosms incubated at 60°C with FeS. Normalized to 1 gram of solid.

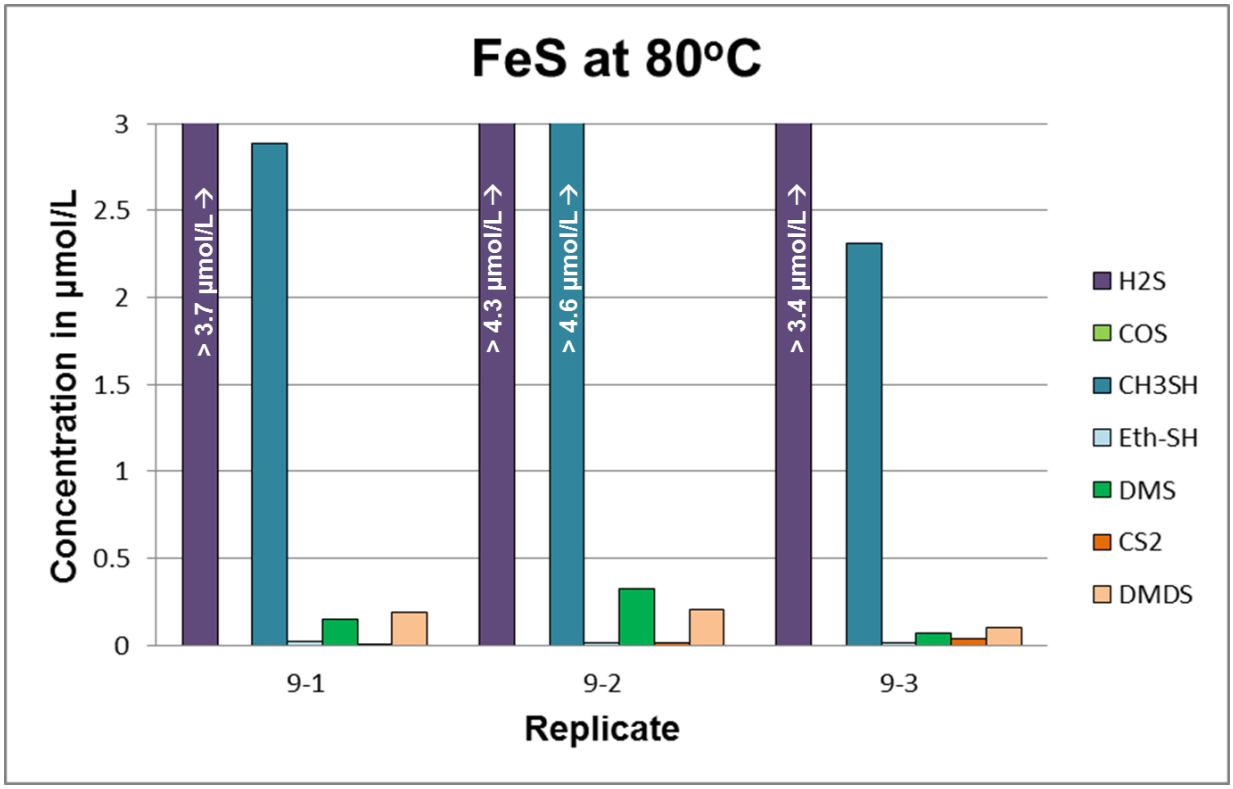

Figure 35: Gases detected in anaerobic microcosms incubated at 80°C with FeS. Normalized to 1 gram of solid.

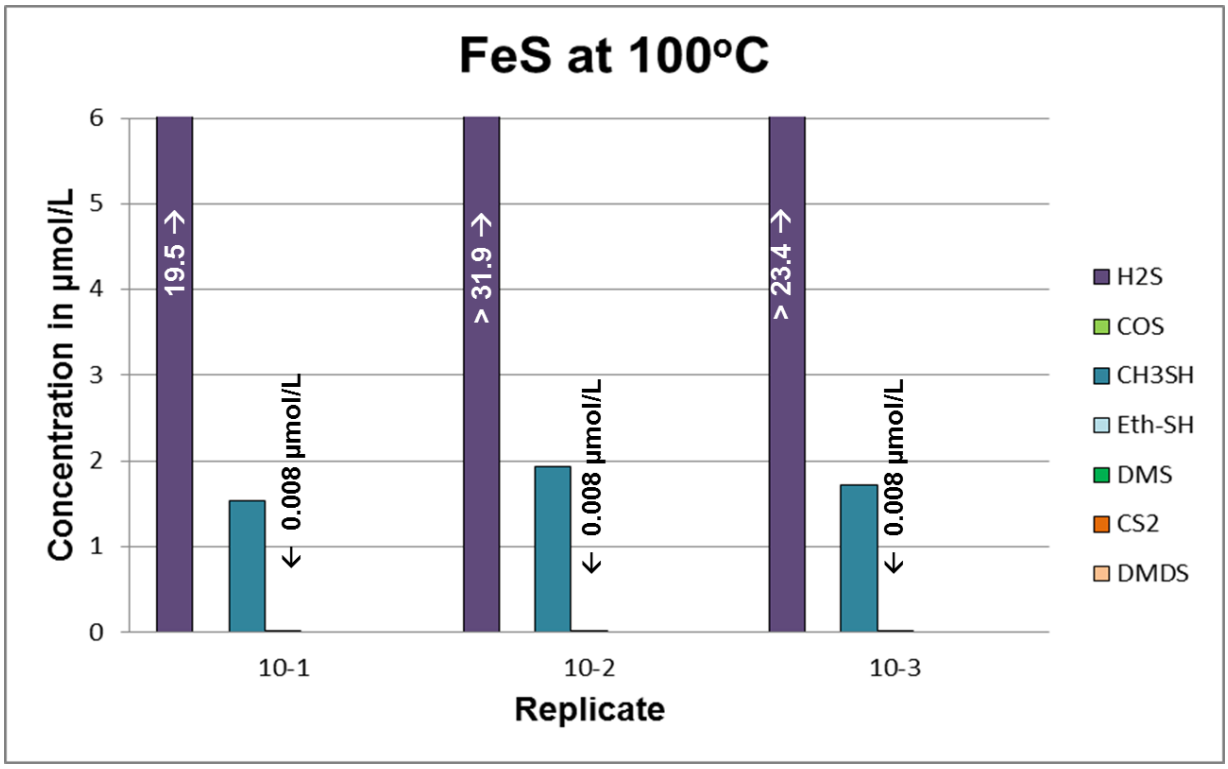

Figure 36: Gases detected in anaerobic microcosms incubated at 100°C with FeS. Normalized to 1 gram of solid.

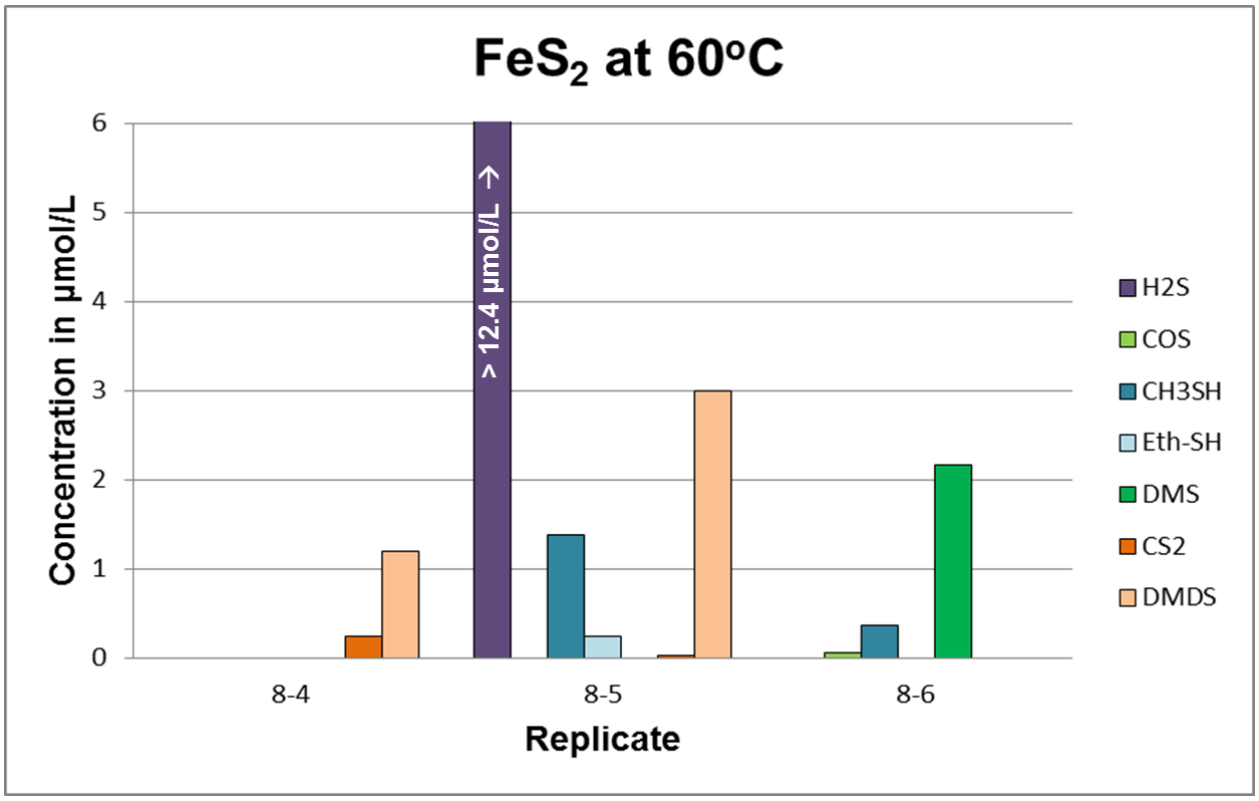

Figure 37: Gases detected in anaerobic microcosms incubated at 60°C with pyrite. Normalized to 1 gram of solid.

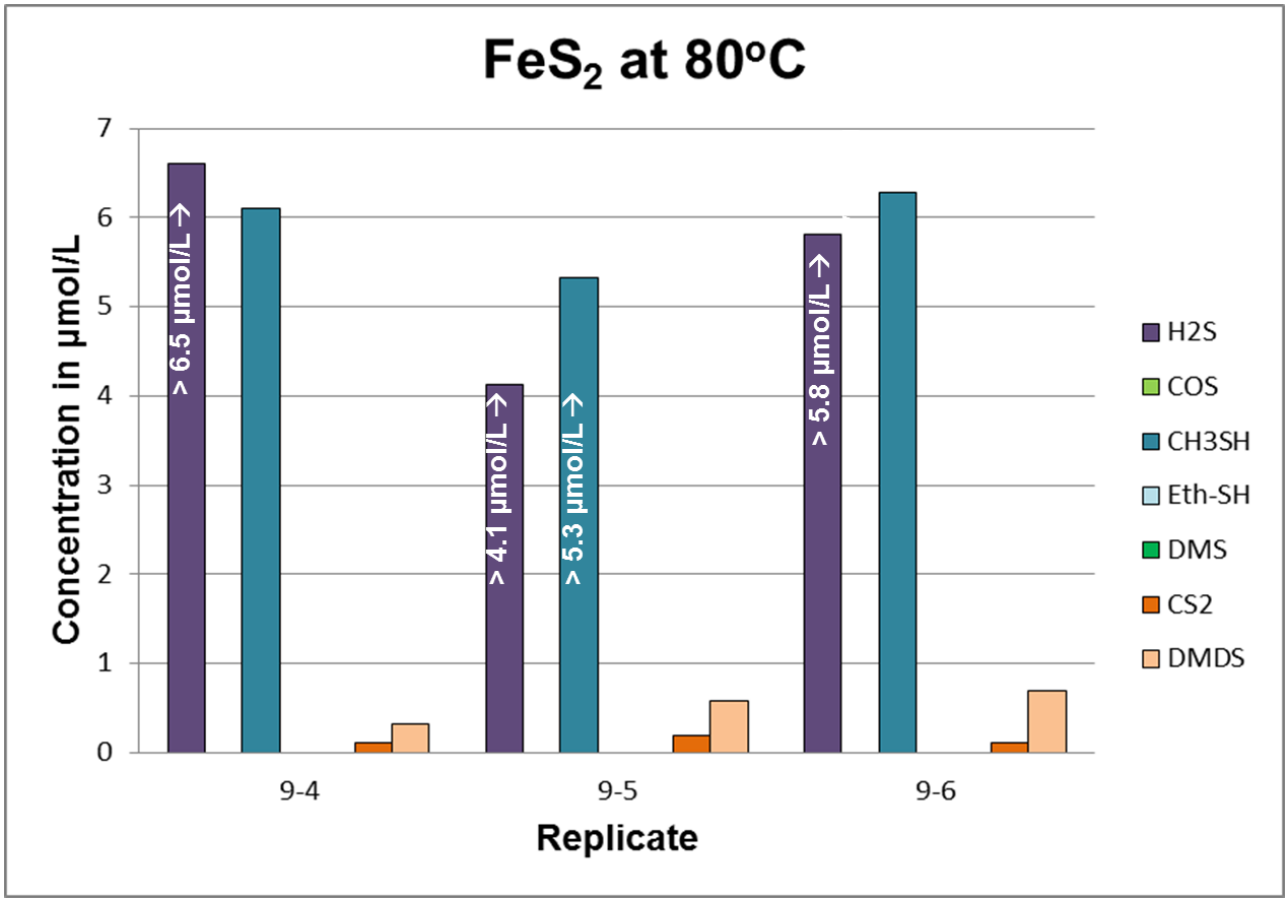

Figure 38: Gases detected in anaerobic microcosms incubated at 80°C with pyrite. Normalized to 1 gram of solid.

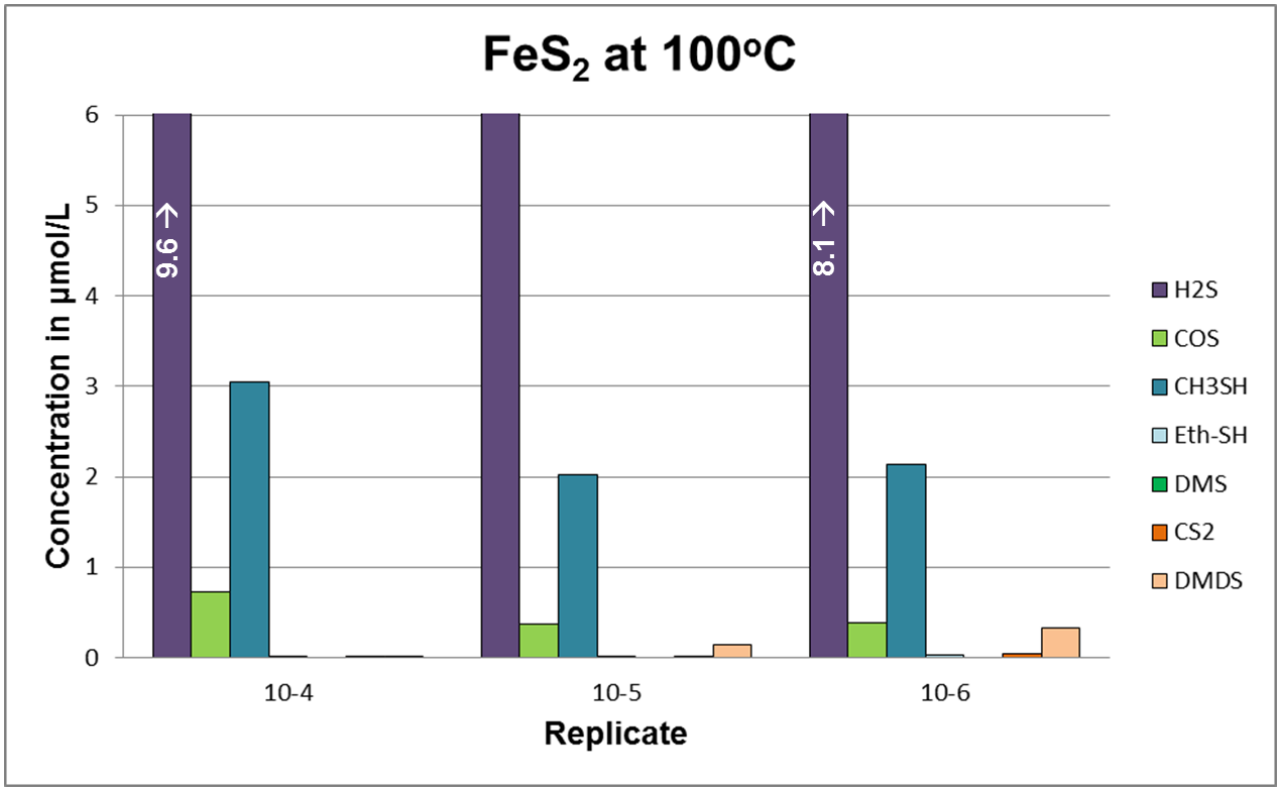

Figure 39: Gases detected in anaerobic microcosms incubated at 100°C with pyrite. Normalized to 1 gram of solid.

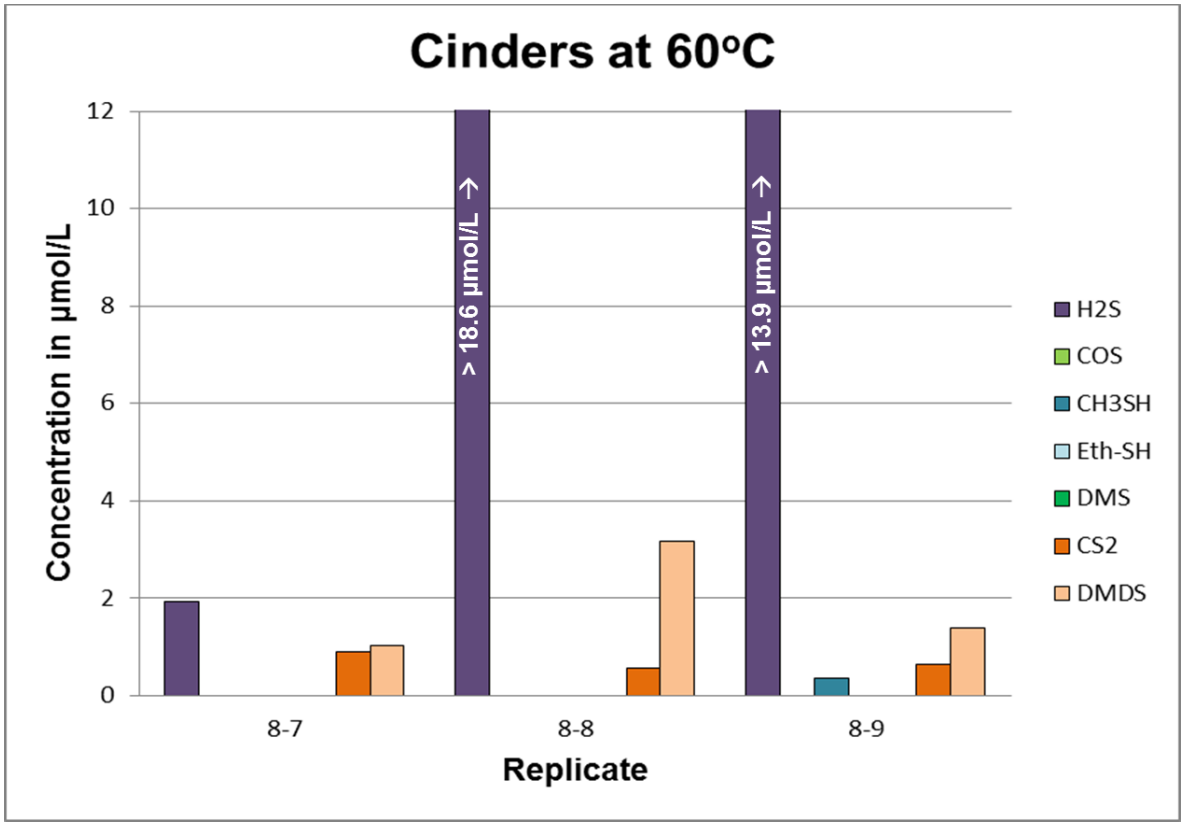

Figure 40: Gases detected in anaerobic microcosms incubated at 60°C with pulverized cinders. Normalized to 1 gram of solid.

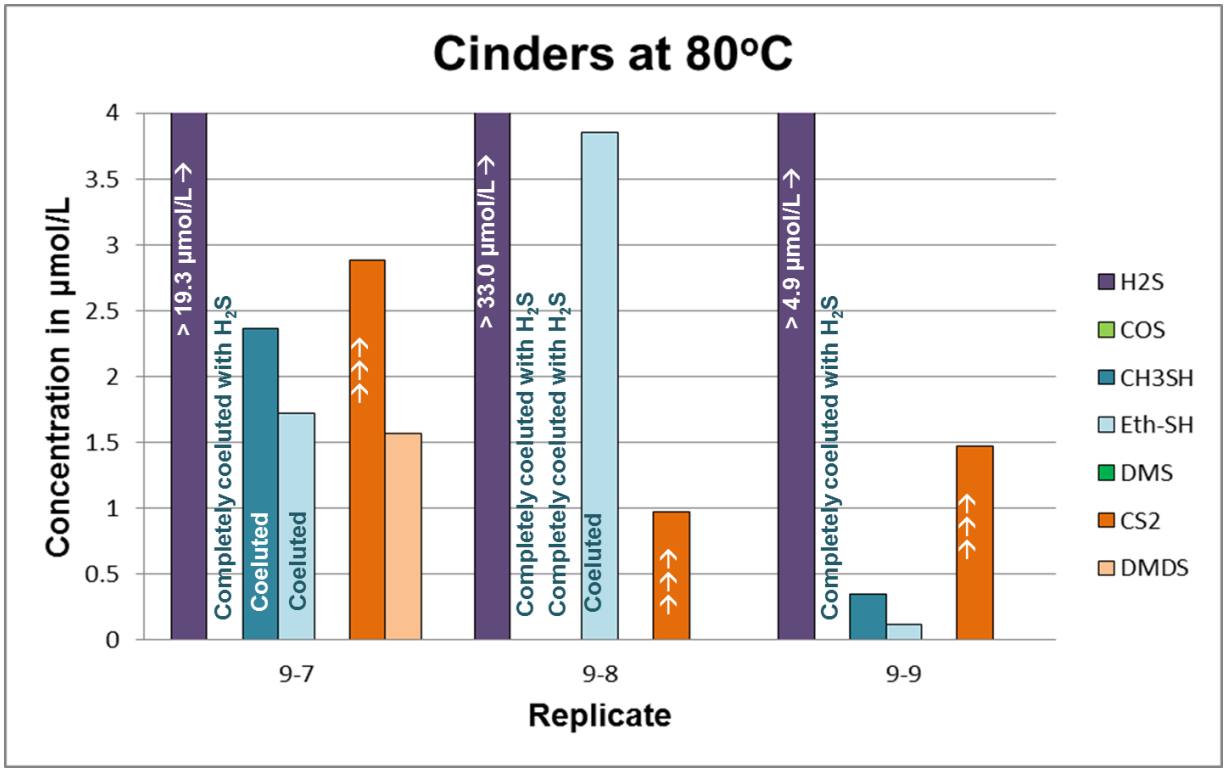

Figure 41: Gases detected in anaerobic microcosms incubated at 80°C with pulverized cinders. Normalized to 1 gram of solid. Arrows indicate that the bar represents a value obtained by integration of the visible portion of an over range peak.

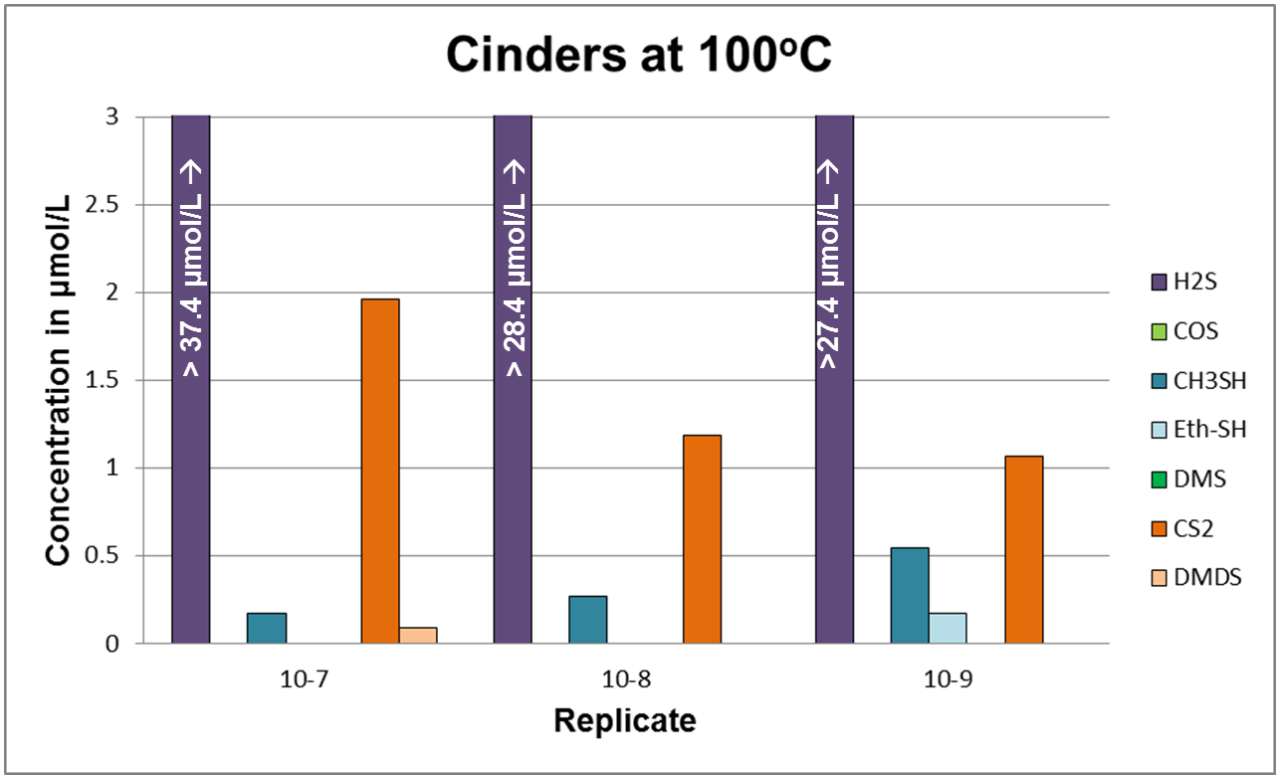

Figure 42: Gases detected in anaerobic microcosms incubated at 100°C with pulverized cinders. Normalized to 1 gram of solid.

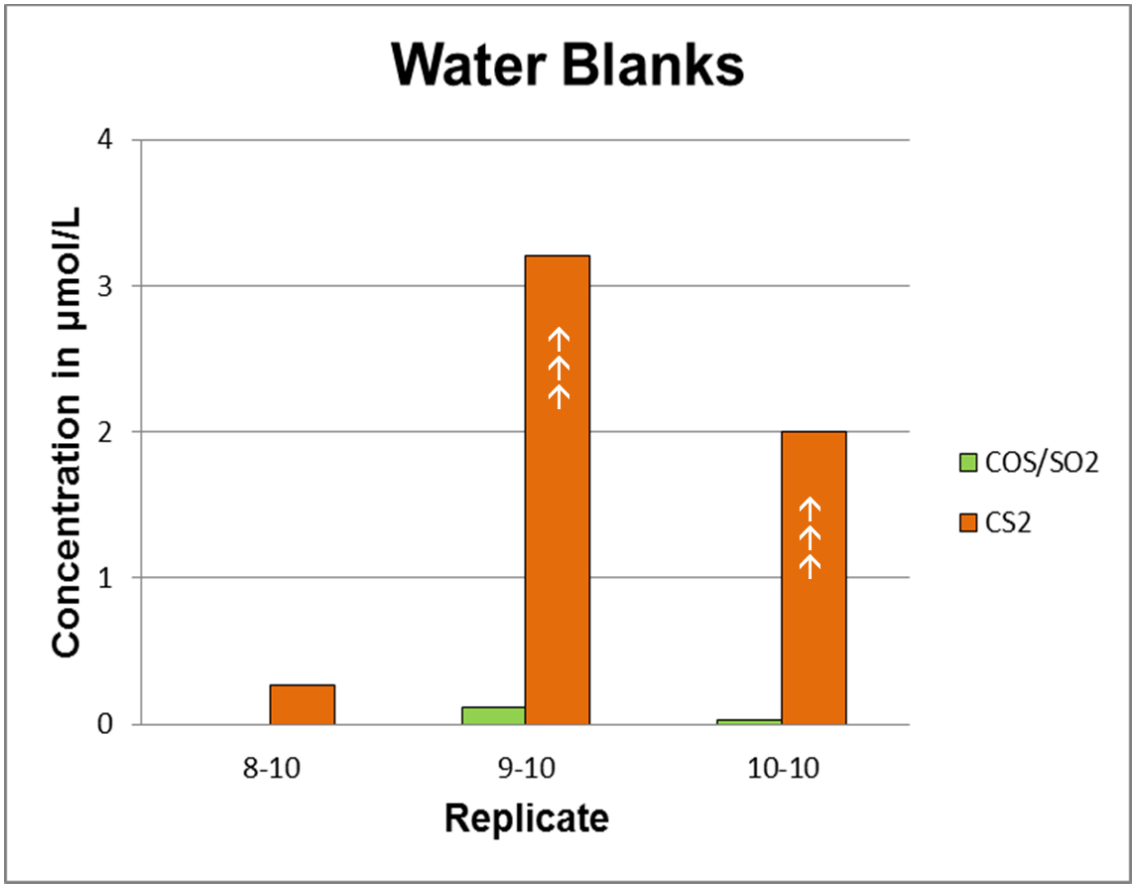

Figure 43: Synthetic Cinder Pool water blanks performed at 60, 80, and 100°C. Arrows indicate that the bar represents a value obtained by integration of the visible portion of an over range peak.

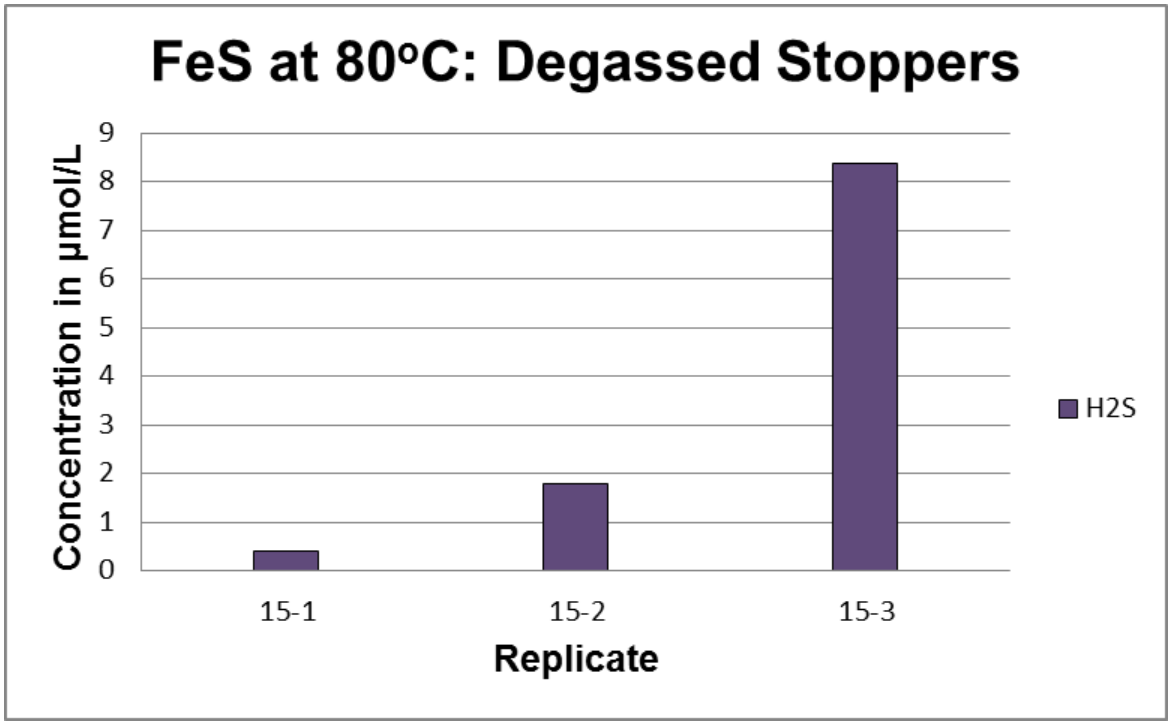

Figure 44: Gases detected in anaerobic microcosms incubated at 80°C with FeS and degassed stoppers. Normalized to 1 gram of solid.

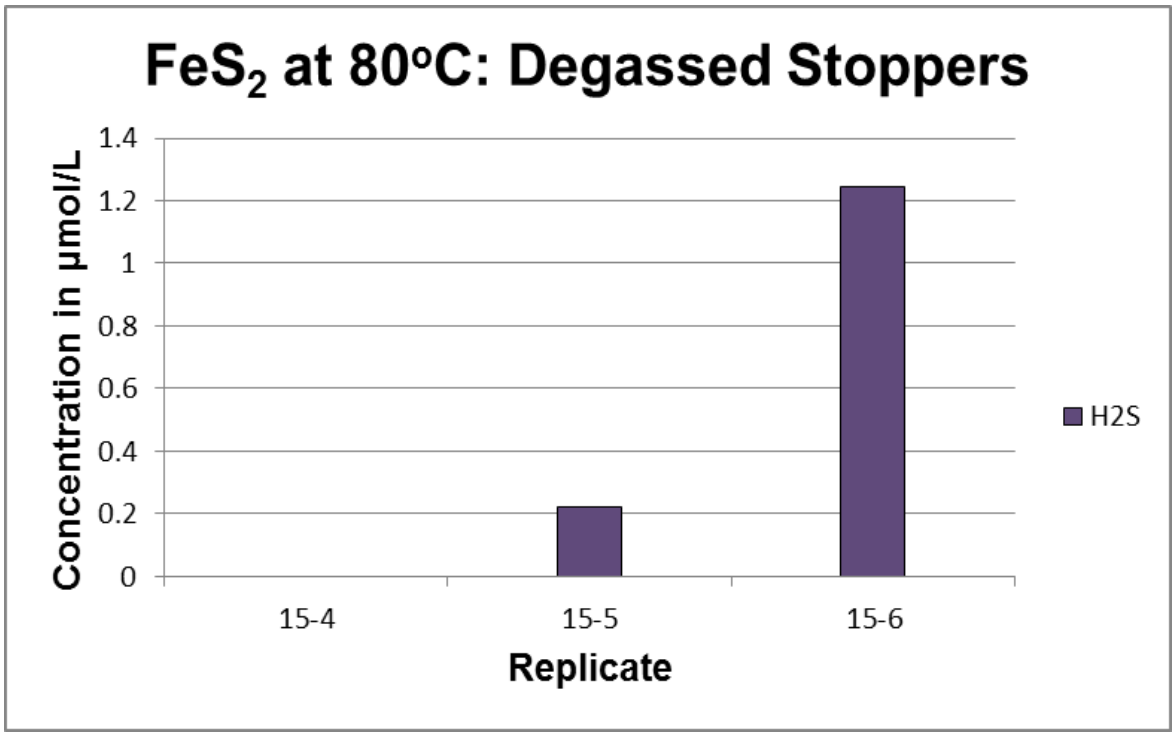

Figure 45: Gases detected in anaerobic microcosms incubated at 80°C with FeS_2 and degassed stoppers. Normalized to 1 gram of solid.

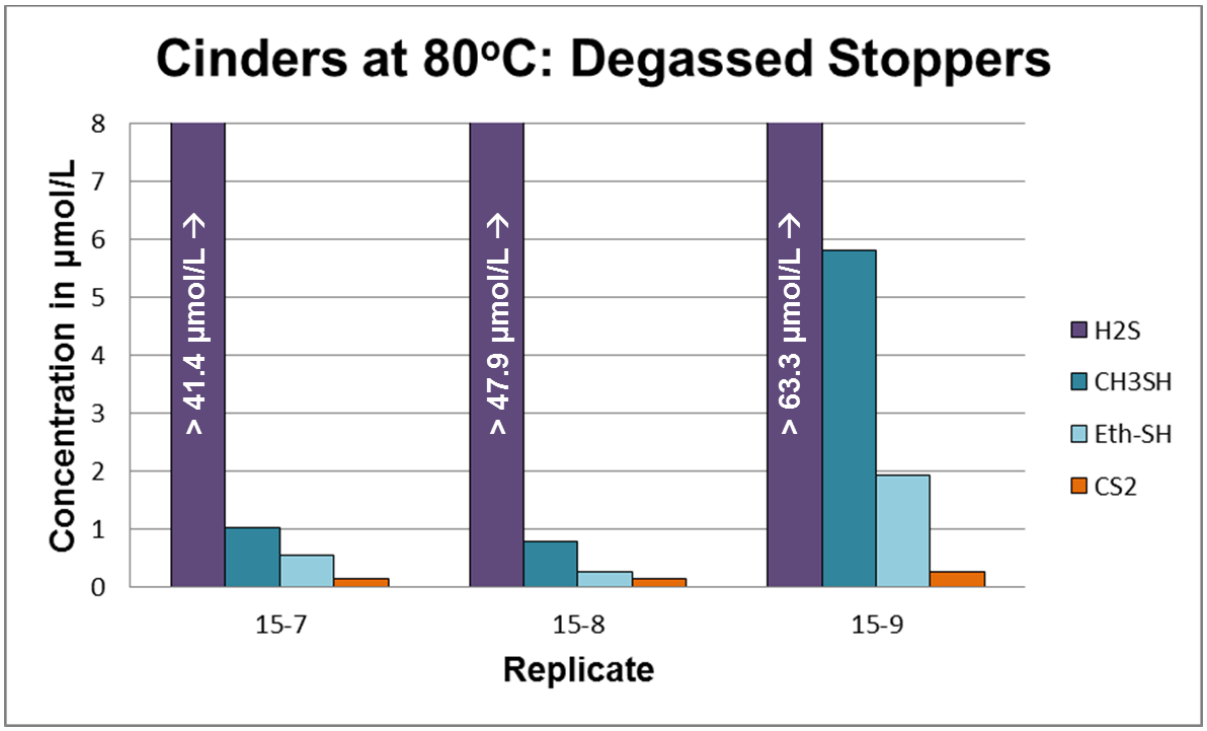

Figure 46: Gases detected in anaerobic microcosms incubated at 80°C with cinders and degassed stoppers. Normalized to 1 gram of solid.

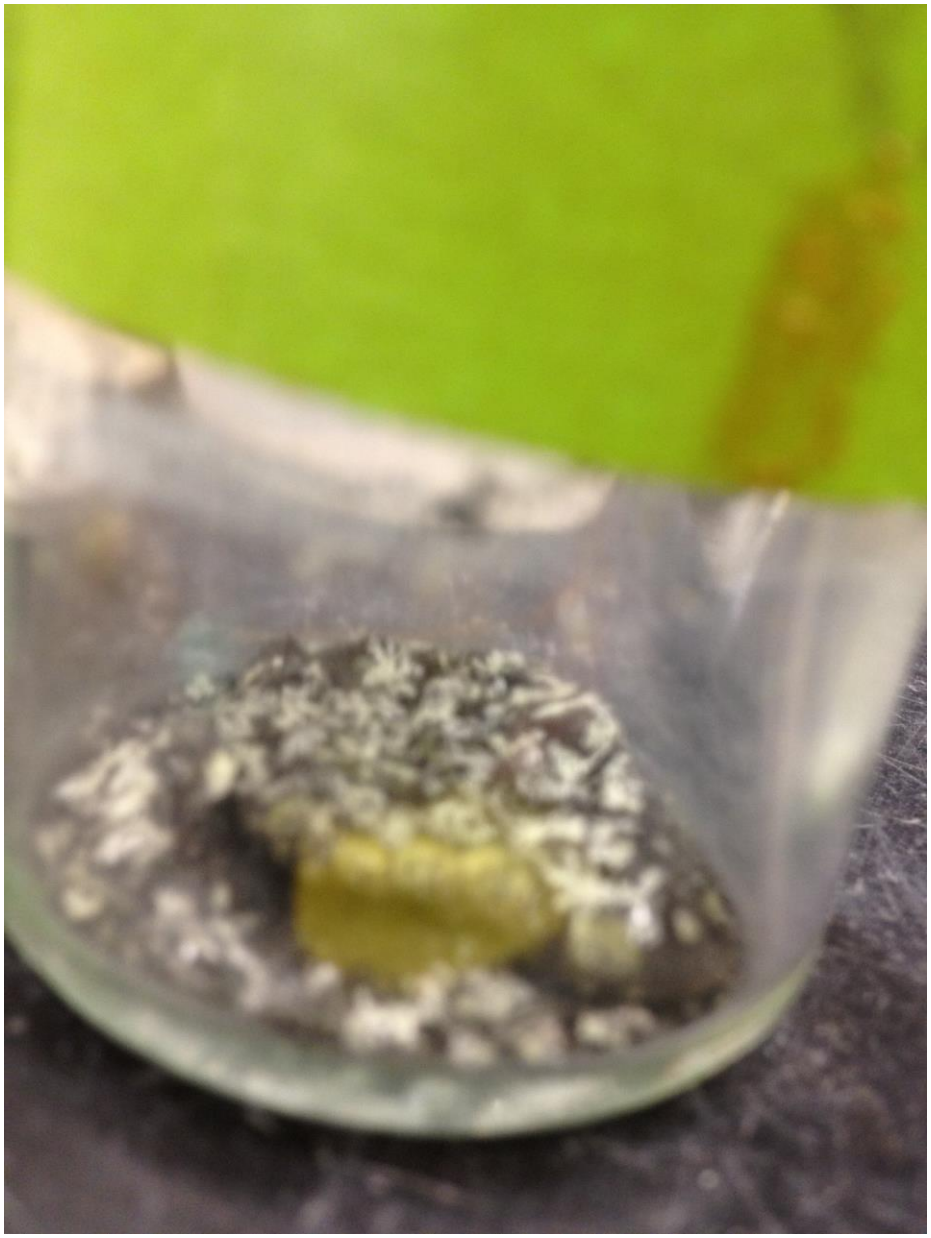

Figure 47: Cinder material after autoclaving. Preferential melting has separated the elemental sulfur from the metal material.

References

Bray CJ, Spooner ETC, Thomas A V (1991) Fluid inclusion volatile analysis by heated crushing , on-line gas chromatography ; applications to Archean fluids. 42:167–193.

Cody GD (2000) Primordial Carbonylated Iron-Sulfur Compounds and the Synthesis of Pyruvate. Science 289:1337–1340.

Dias D, do Nascimento PC, Jost CL, et al. (2010) Voltammetric Determination of Low-Molecular-Weight Sulfur Compounds in Hydrothermal Vent Fluids - Studies with Hydrogen Sulfide, Methanethiol, Ethanethiol and Propanethiol. Electroanalysis 22:1066–1071.

Dimroth E, Kimberley MM (1976) Precambrian atmospheric oxygen: evidence in the sedimentary distributions of carbon, sulfur, uranium, and iron. Canadian Journal of Earth Sciences 13:1161–1185.

Drobner E, Huber H, Wächtershäuser G (1990) Pyrite formation linked with hydrogen evolution under anaerobic conditions. Nature 346:5–6.

eFunda (2013) O Ring Material Suitable for Dry Sulfur Dioxide Gas. http://www.efunda.com/glossary/design/oring/design--oring--chemical--dry_sulfur_dioxide_gas.cfm.

ESI General Information for Butyl Rubber. http://www.elastotechsouthwest.com/butyl.htm.

Gutiérrez OY, Kaufmann C, Hrabar A, et al. (2011) Synthesis of methyl mercaptan from carbonyl sulfide over sulfide K2MoO4/SiO2. Journal of Catalysis 280:264–273.

Heinen W, Lauwers AM (1996) Organic Sulfur Compounds Resulting from the Interaction of Iron Sulfide, Hydrogen Sulfide, and Carbon Dioxide in an Anaerobic Aqueous Environment. Origins of life and evolution of the biosphere : the journal of the International Society for the Study of the Origin of Life 131–150.

Huber C, Wächtershäuser G (1997) Activated Acetic Acid by Carbon Fixation on (Fe,Ni)S Under Primordial Conditions. Science 276:245–247.

Hügler M, Huber H, Molyneaux SJ, et al. (2007) Autotrophic CO2 fixation via the reductive tricarboxylic acid cycle in different lineages within the phylum Aquificae: evidence for two ways of citrate cleavage. Environmental microbiology 9:81–92.

Konhauser K (2007) Introduction to Geomicrobiology. Blackwell Science Ltd

Law J, Phillips N (2006) Witwatersrand gold-pyrite-uraninite deposits do not support a reducing Archean atmosphere. Evolution of Early Earth's Atmosphere, Hydrosphere and Biosphere--Constraints from Ore Deposits

Lomans BP, Maas R, Luderer R, et al. (1999) Isolation and characterization of Methanomethylovorans hollandica gen. nov., sp. nov., isolated from freshwater sediment, a methylotrophic methanogen able to grow on dimethyl sulfide and methanethiol. Applied and environmental microbiology 65:3641–50.

Lomans BP, Smolders a, Intven LM, et al. (1997) Formation of dimethyl sulfide and methanethiol in anoxic freshwater sediments. Applied and environmental microbiology 63:4741–7.

Martin W, Russell MJ (2007) On the origin of biochemistry at an alkaline hydrothermal vent. Philosophical transactions of the Royal Society of London Series B, Biological sciences 362:1887–925.

Mcinnes DM (2003) Bubble Stripping to Determine Hydrogen Concentrations in Ground Water : A Practical Application of Henry ' s Law. Journal of Chemical Education 80:1–4.

Miller SL (1953) A Production of Amino Acids under Possible Primitive Earth Conditions. Science 117

Miller SL, Urey HC (1959) Organic Compound Synthesis on the Primitive Earth. Science 130

NASA Headline News (2001) Life as We Didn't Know It - NASA Science.

Oae S (1992) Organic Sulfur Chemistry: Structure and Mechanism. 212–215.

Oparin AI, Morgulis S (1938) The Origin of Life. Macmillan, New York

Ragsdale SW (1991) Enzymology of the acetyl-CoA pathway of CO2 fixation. Critical reviews in biochemistry and molecular biology 26:261–300.

Reysenbach A-L, Hamamura N, Podar M, et al. (2009) Complete and draft genome sequences of six members of the Aquificales. Journal of bacteriology 191:1992–3.

Rushdi AI, Simoneit BRT (2005) Abiotic Synthesis of Organic Compounds from Carbon Disulfide Under Hydrothermal Conditions. Astrobiology 5

Russell MJ, Hall a J (1997) The emergence of life from iron monosulphide bubbles at a submarine hydrothermal redox and pH front. Journal of the Geological Society 154:377–402.

Sander R (1999) Compilation of Henry ' s Law Constants for Inorganic and Organic Species of Potential Importance in Environmental Chemistry.

Schulte MD, Rogers KL (2004) Thiols in hydrothermal solution: standard partial molal properties and their role in the organic geochemistry of hydrothermal environments. Geochimica et Cosmochimica Acta 68:1087–1097.

Sie BKT (1971) Sulfur Dioxide Formation in the Photo-oxidation of Methanethiol. 1–4.

Spear JR, Walker JJ, McCollom TM, Pace NR (2005) Hydrogen and bioenergetics in the Yellowstone geothermal ecosystem. Proceedings of the National Academy of Sciences of the United States of America 102:2555–60.

Stumm W, Morgan J (1996) Aquatic Chemistry, 3rd ed. Wiley-Interscience

Sturm GP (1969) The Photodissociation of Hydrogen Sulfide and Methanethiol. Wavelength Dependence of the Energy Partition in the Primary Products. The University of Texas at Austin, Austin Texas

Urey HC (1952) On the Early Chemical History of the Earth and the Origin of Life. National Academy of Sciences 38

Wächtershäuser G (1990a) The Case for the Chemoautotropic Origin of Life. Origins of Life and Evolution of the Biosphere 173–176.

Wächtershäuser G (1988a) Pyrite formation, the first energy source for life: a hypothesis. Systematic and Applied Microbiology 10:207–210.

Wächtershäuser G (1988b) Before Enzymes and Templates: Theory of Surface Metabolism. Microbiological Reviews 52:452–484.

Wächtershäuser G (1990b) Evolution of the first metabolic cycles. Proceedings of the National Academy of Sciences of the United States of America 87:200–4.

Wächtershäuser G (2007) On the Chemistry and Evolution of the Pioneer Organism. Chemistry and Biodiversity 4:584–602.

Wächtershäuser G (1994) Life in a ligand sphere. Proceedings of the National Academy of Sciences of the United States of America 91:4283–7.

Xu Y, Schoonen MAA, Nordstrom DK, et al. (2000) Sulfur geochemistry of hydrothermal waters in Yellowstone National Park, Wyoming, USA. II. Formation and decomposition of thiosulfate and polythionate in Cinder Pool. Journal of Volcanology and Geothermal Research 97:407–423.

Vita

Lindsey Allison Sydow was born and raised in San Marcos, Texas with a fascination for the natural world. She graduated near the top of her class from San Marcos High School in 2005. Lindsey went on to attend Texas A&M University and graduated Cum Laude with a B.S. in Environmental Geoscience in 2009. After working at the University of Idaho as part of the National Science Foundation's REU program in 2009, she decided to attend graduate school at the University of Texas at Austin.

Contact at lasydow@gmail.com

This thesis was typed by Lindsey Allison Sydow